Global performance of the state-of-the-art covariant energy density functionals and related theoretical uncertainties

Anatoli Afanasjev

Mississippi State University (MSU), USA

1. Motivation: better understanding of the accuracy and uncertainties in the description of different observables and how they propagate to nuclear extremes
2. Ground state observables (global view)
3. The uncertainties in the predictions and their sources
   - neutron-drip line
   - superheavy nuclei
4. Single-particle properties: a key role
5. Conclusions

In collaboration with S.Abgemava, D. Ray (MSU), P. Ring (TU Munich) and T. Nakatsukasa (Tsukuba U) and E. Litvinova (WMU)

Collective degrees of freedom (deformation, rotation, fission)

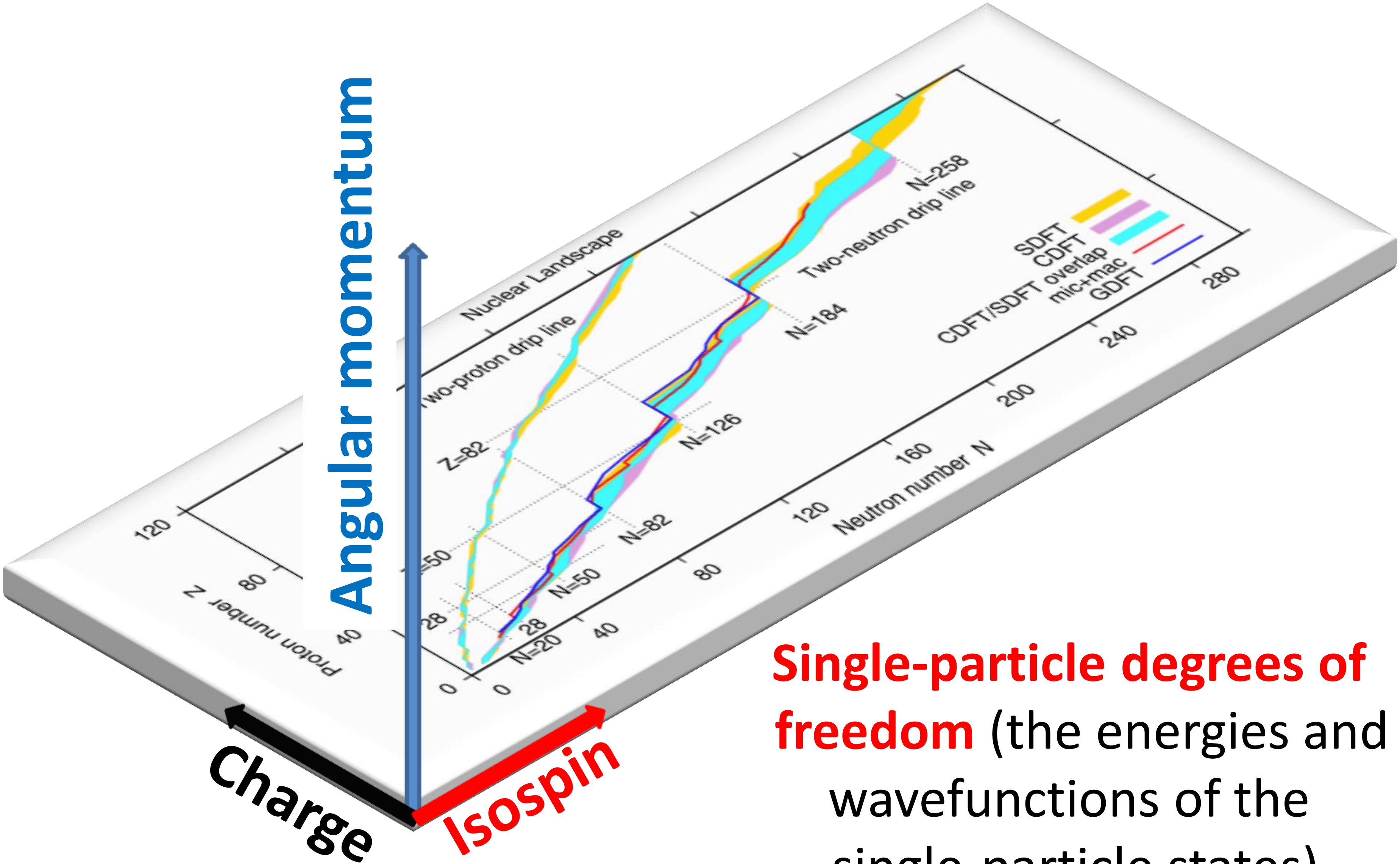

Single-particle degrees of freedom (the energies and wavefunctions of the single-particle states)

1. Motivation: better understanding of the accuracy and uncertainties in the description of different observables and how they propagate to nuclear extremes

Number of the functionals:

Skyrme	– 240	M.Dutra et al, PRC 85, 035201 (2012)
covariant functionals	-- 263,	M. Dutra et al, PRC 90, 055203 (2014)

Estimating theoretical errors:

statistical errors - well defined (not yet done)

systematic (non-statistical) errors – well defined for the regions where experimental data exist [remember "error is a deviation from true value" (webster)]

-- not well defined for the regions beyond experimentally known

Theoretical uncertainties are defined by the **spread** (the difference between maximum and minimum values of physical observable obtained with employed set of CEDF's).

$$\Delta O(Z,N) = |O_{\max}(Z,N) - O_{\min}(Z,N)|$$

NL3*, DD-ME2, DD-MEδ, DD-PC1 [also PC-PK1 in superheavy nuclei]

Covariant density functional theory (CDFT)

The nucleons interact via the exchange of effective mesons →
→ **effective Lagrangian**

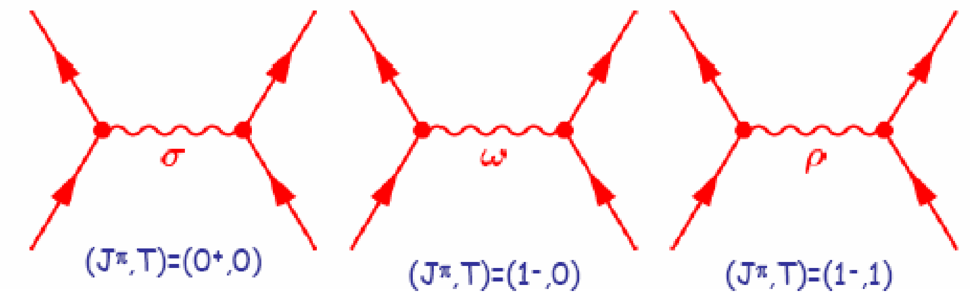

Long-range attractive scalar field

Short-range repulsive vector field

Isovector field

$$E_{\mathrm{RMF}}[\hat{\rho}, \phi_m] = \mathrm{Tr}[(\boldsymbol{\alpha p} + \beta m)\hat{\rho}] \pm \int \left[\frac{1}{2}(\nabla\phi_m)^2 + U(\phi_m)\right] \mathrm{d}^3 r + \mathrm{Tr}[(\Gamma_m \phi_m)\hat{\rho}]$$

density matrix $\hat{\rho}$

$\phi_m \equiv \{\sigma, \omega^\mu, \vec{\rho}^\mu, A^\mu\}$ - meson fields

$$\boxed{\hat{h} = \frac{\delta E}{\delta \hat{\rho}}}$$ **Mean field**

$$\boxed{\hat{h}|\varphi_i\rangle = \varepsilon_i|\varphi_i\rangle}$$ **Eigenfunctions**

Three classes of CDFT models.

Meson-exchange models

$$\mathcal{L} = \bar{\psi}[\gamma(i\partial - g_\omega \omega - g_\rho \vec{\rho}\,\vec{\tau} - eA) - m - g_\sigma \sigma]\psi$$
$$+ \frac{1}{2}(\partial\sigma)^2 - \frac{1}{2}m_\sigma^2\sigma^2 - \frac{1}{4}\Omega_{\mu\nu}\Omega^{\mu\nu} + \frac{1}{2}m_\omega^2\omega^2$$
$$- \frac{1}{4}\vec{R}_{\mu\nu}\vec{R}^{\mu\nu} + \frac{1}{2}m_\rho^2\vec{\rho}^{\,2} - \frac{1}{4}F_{\mu\nu}F^{\mu\nu},$$

Non-linear models

$$U(\sigma) = \frac{1}{2}m_\sigma^2\sigma^2 + \frac{1}{3}g_2\sigma^3 + \frac{1}{4}g_3\sigma^4$$

NL3*

Models with explicit density dependence

no nonlinear terms in the *σ meson*

$$g_i(\rho) = g_i(\rho_{\rm sat}) f_i(x) \quad \text{for} \quad i = \sigma, \omega, \rho$$

$$f_i(x) = a_i \frac{1 + b_i(x + d_i)^2}{1 + c_i(x + d_i)^2}$$ for *σ and ω*

$$f_\rho(x) = \exp[-a_\rho(x - 1)]$$ for *ρ*

$$x = \rho / \rho_{sat}$$

DD-ME2, DD-MEδ

Effective density dependence:

The basic idea comes from ab initio calculations.
Density dependent coupling constants include
Brueckner correlations and three-body forces

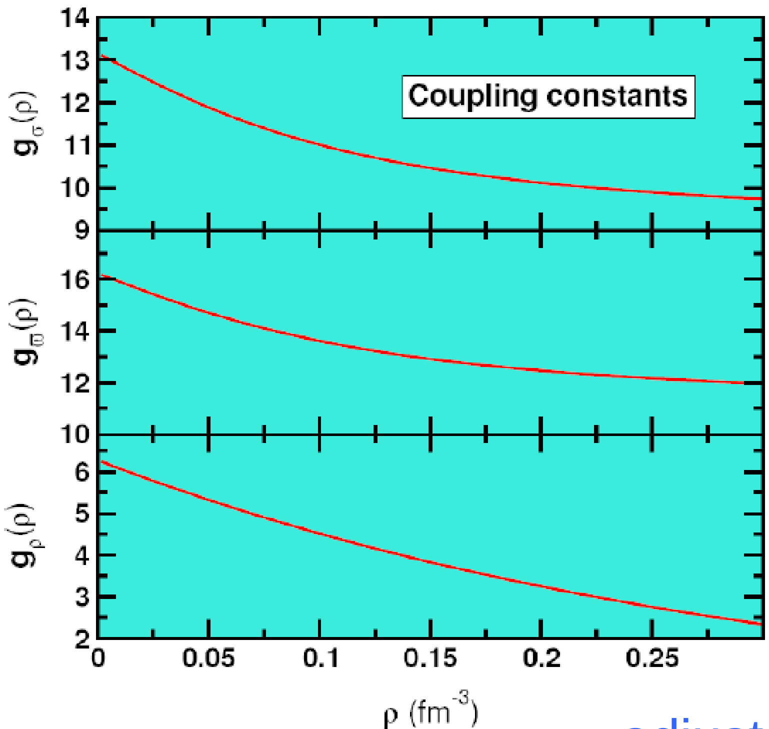

Effective interactions with medium-dependent couplings:

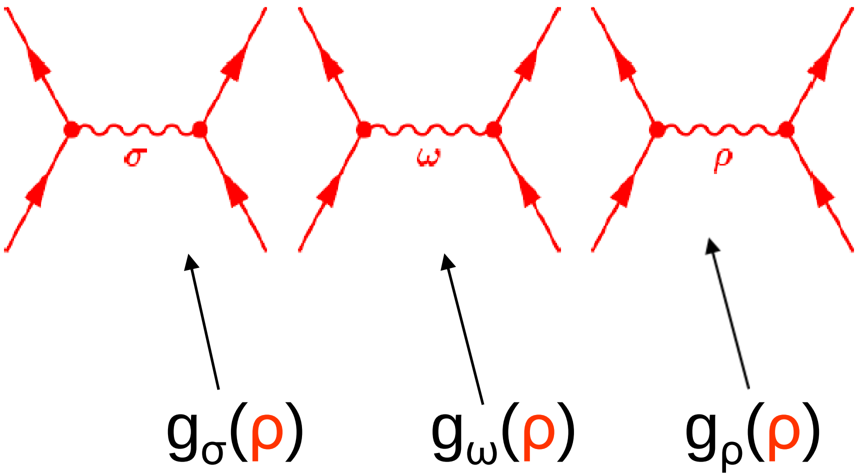

adjusted to ground state properties of finite nuclei

Typel, Wolter, NPA **656**, 331 (1999)
Niksic, Vretenar, Finelli, P.R., PRC **66**, 024306 (2002): **DD-ME1**
Lalazissis, Niksic, Vretenar, P.R., PRC 78, 034318 (2008): **DD-ME2**

Effective density dependence:

The basic idea comes from ab initio calculations.
Sensity dependent coupling constants include
Brueckner correlations and three-body forces

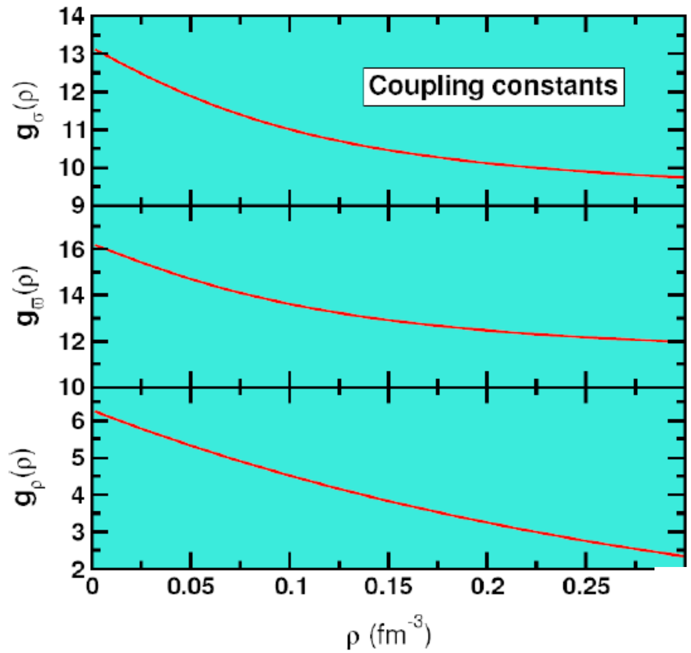

Point-coupling models
with derivative terms:

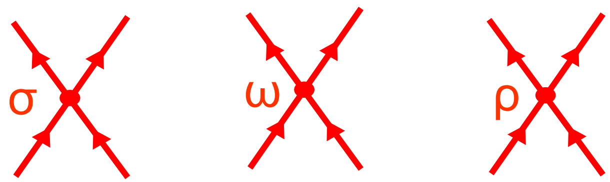

$g_\sigma(\rho)$ $g_\omega(\rho)$ $g_\rho(\rho)$

adjusted to ground state properties of finite nuclei

Manakos and Mannel, Z.Phys. **330**, 223 (1988)
Bürvenich, Madland, Maruhn, Reinhard, PRC **65**, 044308 (2002): **PC-F1**
Niksic, Vretenar, P.R., PRC 78, 034318 (2008): **DD-PC1**
Zhao, Li, Yao, Meng, J. Meng, archiv 1002.1789 **PC-PK1**

Three classes of CDFT models.

Point-coupling models

$$
\begin{aligned}
\mathcal{L} = & \bar{\psi}(i\gamma \cdot \partial - m)\psi \\
& - \frac{1}{2}\alpha_S(\hat{\rho})(\bar{\psi}\psi)(\bar{\psi}\psi) - \frac{1}{2}\alpha_V(\hat{\rho})(\bar{\psi}\gamma^\mu\psi)(\bar{\psi}\gamma_\mu\psi) \\
& - \frac{1}{2}\alpha_{TV}(\hat{\rho})(\bar{\psi}\vec{\tau}\gamma^\mu\psi)(\bar{\psi}\vec{\tau}\gamma_\mu\psi) \\
& - \frac{1}{2}\delta_S(\partial_v\bar{\psi}\psi)(\partial^v\bar{\psi}\psi) - e\bar{\psi}\gamma \cdot A\frac{(1-\tau_3)}{2}\psi .
\end{aligned}
$$

DD-PC1

Details:
1. No mesons
2. The derivative terms account for the leading effects of finite-range interaction,
3. Explicit density dependence

Global performance

Ground state observables: S.E.Agbemava, AA, D.Ray and P.Ring, PRC **89**, 054320 (2014) (37 pages)
includes as a supplement to the manuscript
complete mass, deformation and radii table for even-even nuclei with Z<104 obtained with DD-PC1

Neutron drip lines and sources of their uncertainties:
PLB 726, 680 (2013), PRC **89**, 054320 (2014) , PRC 91, 014324 (2015)

Superheavy nuclei reexamined
AA. S.E.Agbemava, Acta Physica Polonica, 46, 405 (2015)
S.E.Agbemava, AA, T. Nakatsukasa, P. Ring, PRC 92, 054310 (2015)
includes as a supplement to the manuscript
complete mass, deformation and radii table for even-even nuclei with 106<Z<130 obtained with DD-PC1 and PC-PK1

Systematic studies in local regions (mostly actinides)

Accuracy of the description of deformed one-quasiparticle states

AA and S.Shawaqfeh, PLB 706 (2011) 177

Fission barriers in actinides and SHE

actinides: H. Abusara, AA and P. Ring, PRC 82, 044303 (2010)

superheavies: H. Abusara, AA and P. Ring, PRC 85, 024314 (2012)

and to be published

Pairing and rotational properties of even-even of odd-mass actinides

AA and O.Abdurazakov, PRC 88, 014320 (2013),

AA, Phys. Scr. 89 (2014) 054001

2. Ground state observables (global view)

RHB framework

$$\begin{pmatrix} h_D - \lambda & \Delta \\ -\Delta^* & -h_D^* + \lambda \end{pmatrix} \begin{pmatrix} U \\ V \end{pmatrix}_k = E_k \begin{pmatrix} U \\ V \end{pmatrix}_k$$

1. Axial RHB calculations in large basis (all fermionic states up to N_F=20 and bosonic states up to N_B=20 are included)

2. The separable version of the finite range Brink-Booker part of the Gogny D1S force is used in the particle-particle channel; its strength variation across the nuclear chart is defined by means of the fit of rotational moments of inertia calculated in the cranked RHB framework to experimental data.

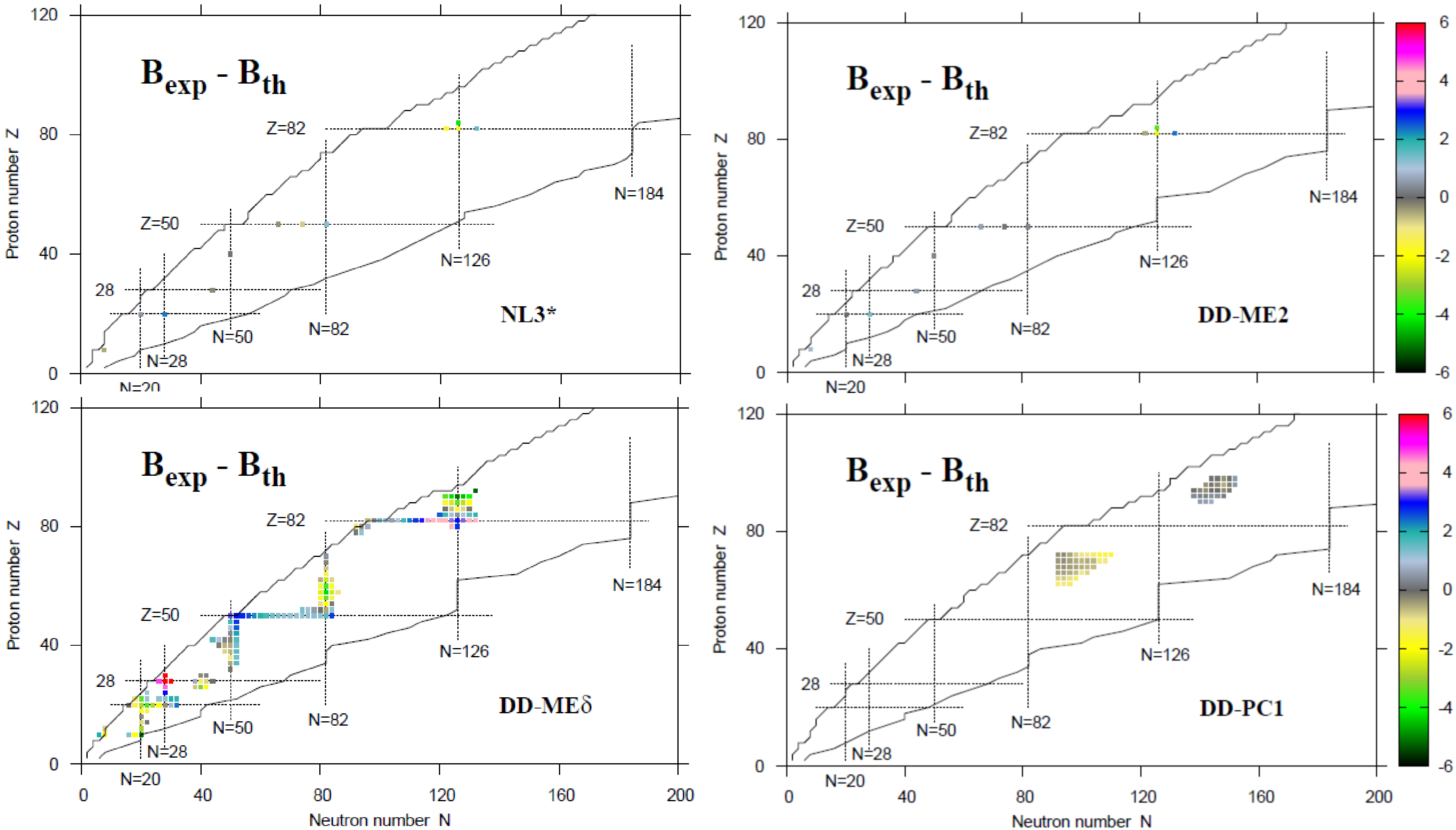

NL3*- G.A. Lalazissis et al PLB 671 (2009) 36 - **7 parameters**

DD-ME2 - G. A. Lalazissis, et al, PRC **71**, 024312 (2005) – **10 parameters**

DD-PC1 - T. Niksic et al, PRC **78**, 034318 (2008) – **10 parameters**

DD-Meδ - X. Roca-Maza et al, PRC **84**, 054309 (2011) – **14 parameters**

only 4 parameters are fitted to finite nuclei,

others - to Bruckner calculations of nuclear matter

What are theoretical uncertainties in the description of experimental masses

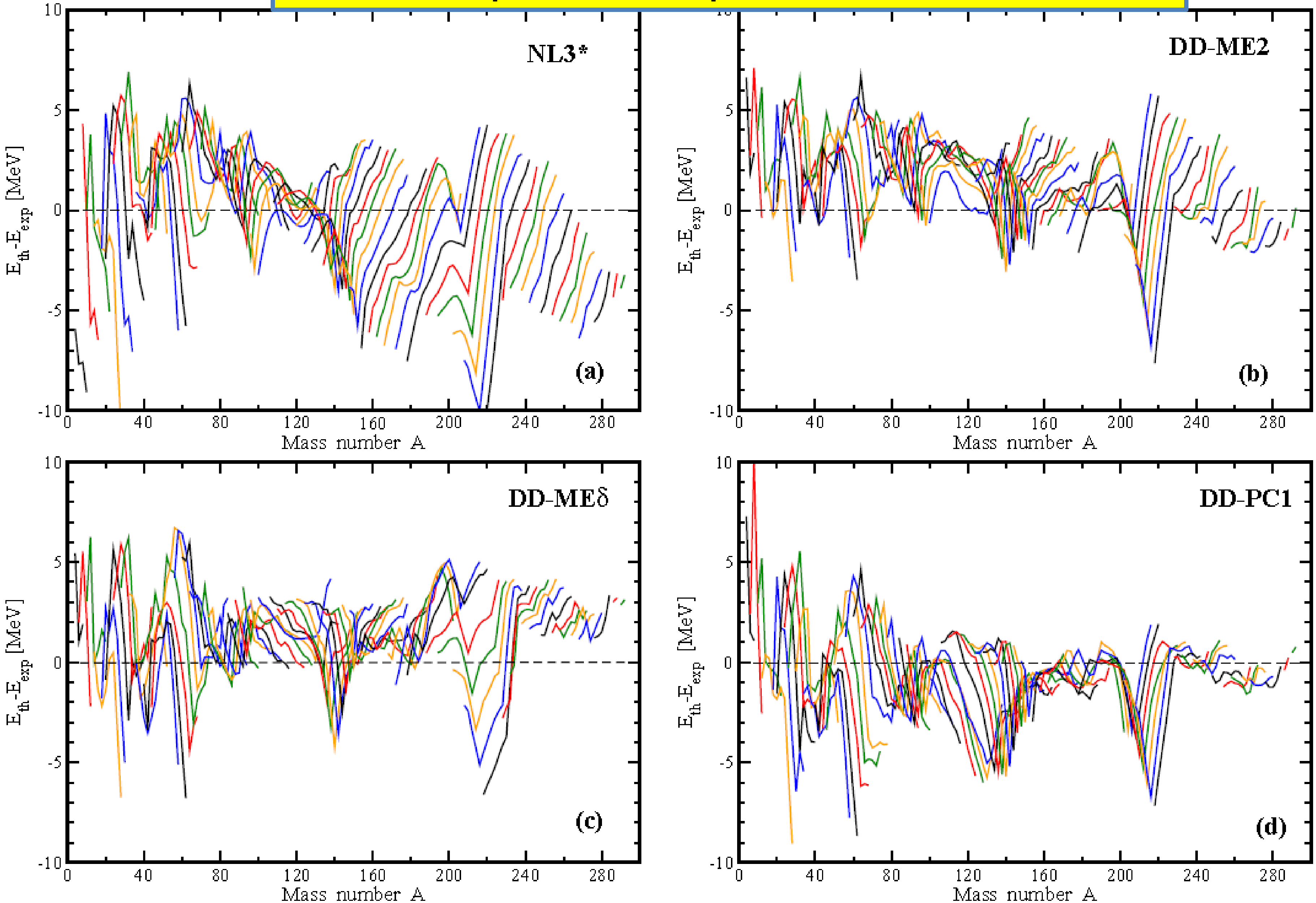

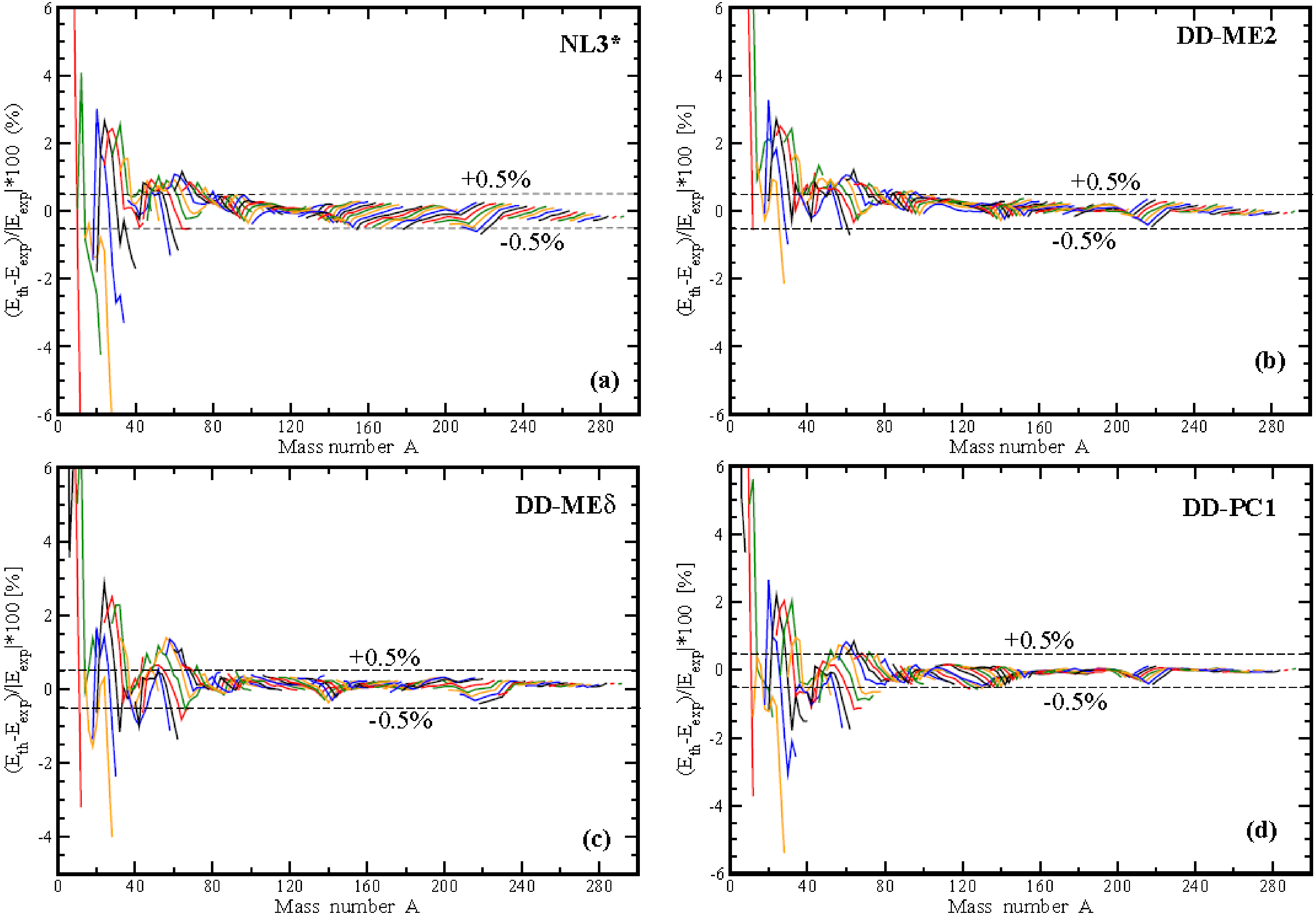
NL3*
DD-ME2
DD-MEδ
DD-PC1
(a)
(b)
(c)
(d)
+0.5%
-0.5%
$(E_{th}-E_{exp})/|E_{exp}|*100$ (%)
$(E_{th}-E_{exp})/|E_{exp}|*100$ [%]
Mass number A

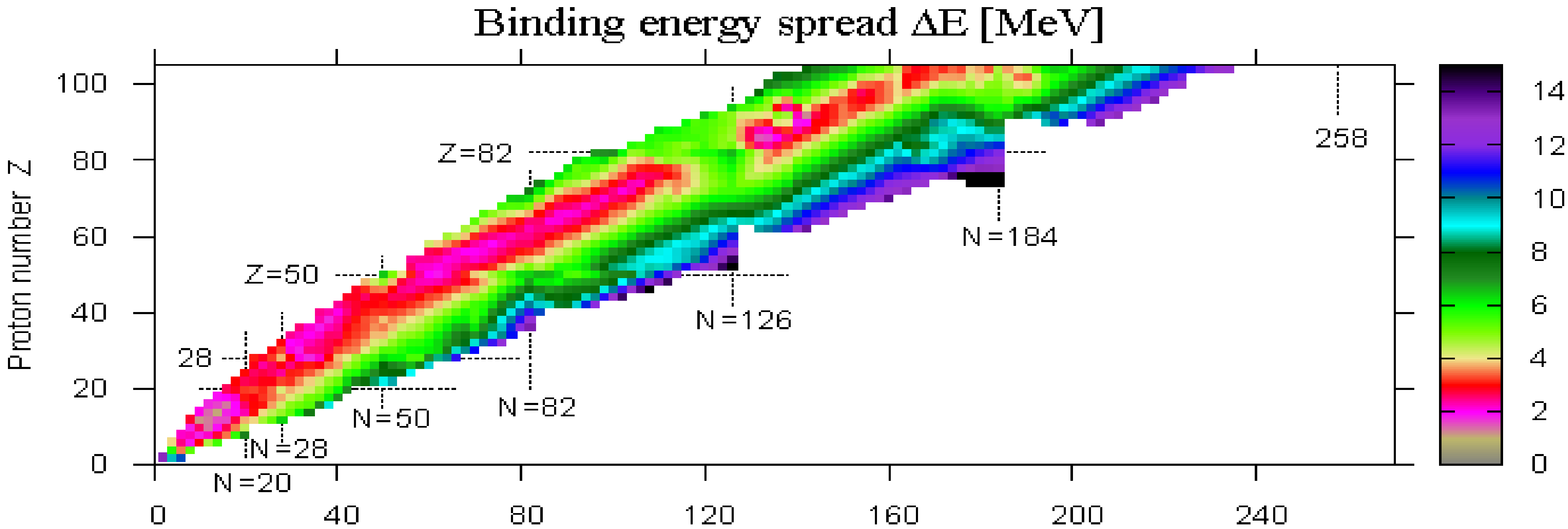

Propagation of theoretical uncertainties in masses with isospin

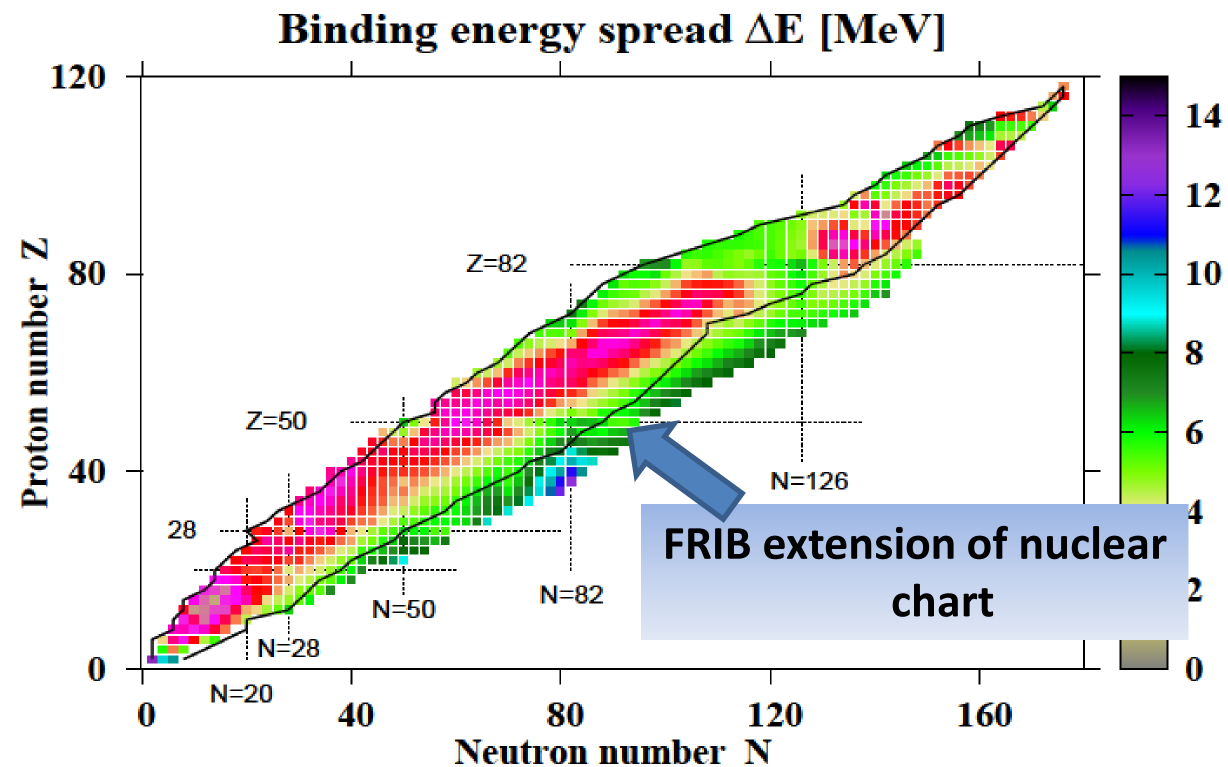

Nuclear matter properties and propagation of the mass uncertainties towards neutron drip line

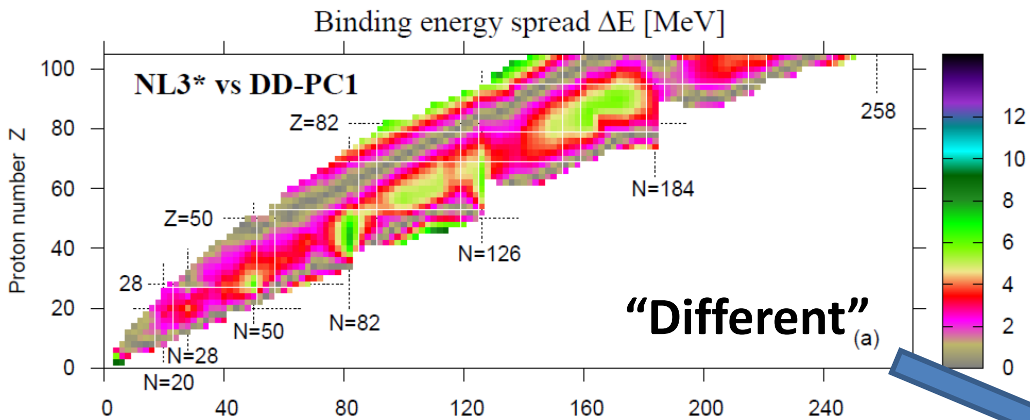

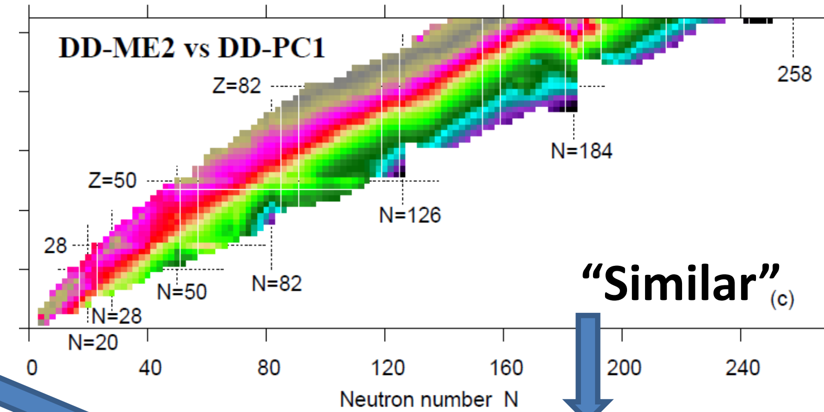

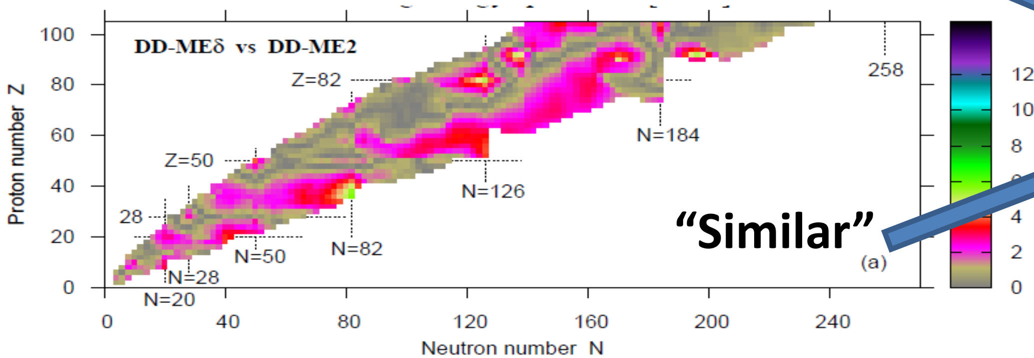

nuclear matter properties

NMP do not allow to reduce the uncertainties towards neutron drip line

CEDF	ρ_0 [fm^{-3}]	E/A [MeV]	K_∞ [MeV]	J [MeV]	L [MeV]	m^*/m	ΔE_{rms} [MeV]
1	2	3	4	5	6	7	8
NL3* [4]	0.150	-16.31	258	**38.68**	**122.6**	0.67	2.96
DD-ME2 [5]	0.152	-16.14	251	32.40	49.4	0.66	2.39
DD-MEδ [10]	0.152	-16.12	219	32.35	52.9	0.61	2.29
DD-PC1 [11, 12]	0.152	-16.06	230	33.00	68.4	0.66	2.01
PC-PK1 [12]	0.154	-16.12	238	**35.6**	**113**	0.65	2.58

TABLE III. The rms-deviations ΔE_{rms}, $\Delta(S_{2n})_{\mathrm{rms}}$ ($\Delta(S_{2p})_{\mathrm{rms}}$) between calculated and experimental binding energies E and two-neutron(-proton) separation energies S_{2n} (S_{2p}). They are given in MeV for the indicated CDFT parameterizations with respect to "measured" and "measured+estimated" sets of experimental masses.

EDF	measured	measured+estimated		
	ΔE_{rms}	ΔE_{rms}	$\Delta(S_{2n})_{\mathrm{rms}}$	$\Delta(S_{2p})_{\mathrm{rms}}$
NL3*	2.96	3.00	1.23	1.29
DD-ME2	2.39	2.45	1.05	0.95
DD-MEδ	2.29	2.40	1.09	1.09
DD-PC1	2.01	2.15	1.16	1.03

RMF+BCS results (FSUGold, NL3, TM1, BSR4)
P.-G. Reinhard et al, Int. J. Mod. Phys. E20, 1379 (2011)

UNEDF* - Kortelainen et al, PRC 89, 054314 (2015)

Force	**ΔErms [MeV]**
FSUGold	6.5
NL3	3.8
TM1	5.9
BSR4	2.6
Skyrme DFT	
UNEDF1	1.91
UNEDF2	1.95

Theoretical uncertainties in charge radii

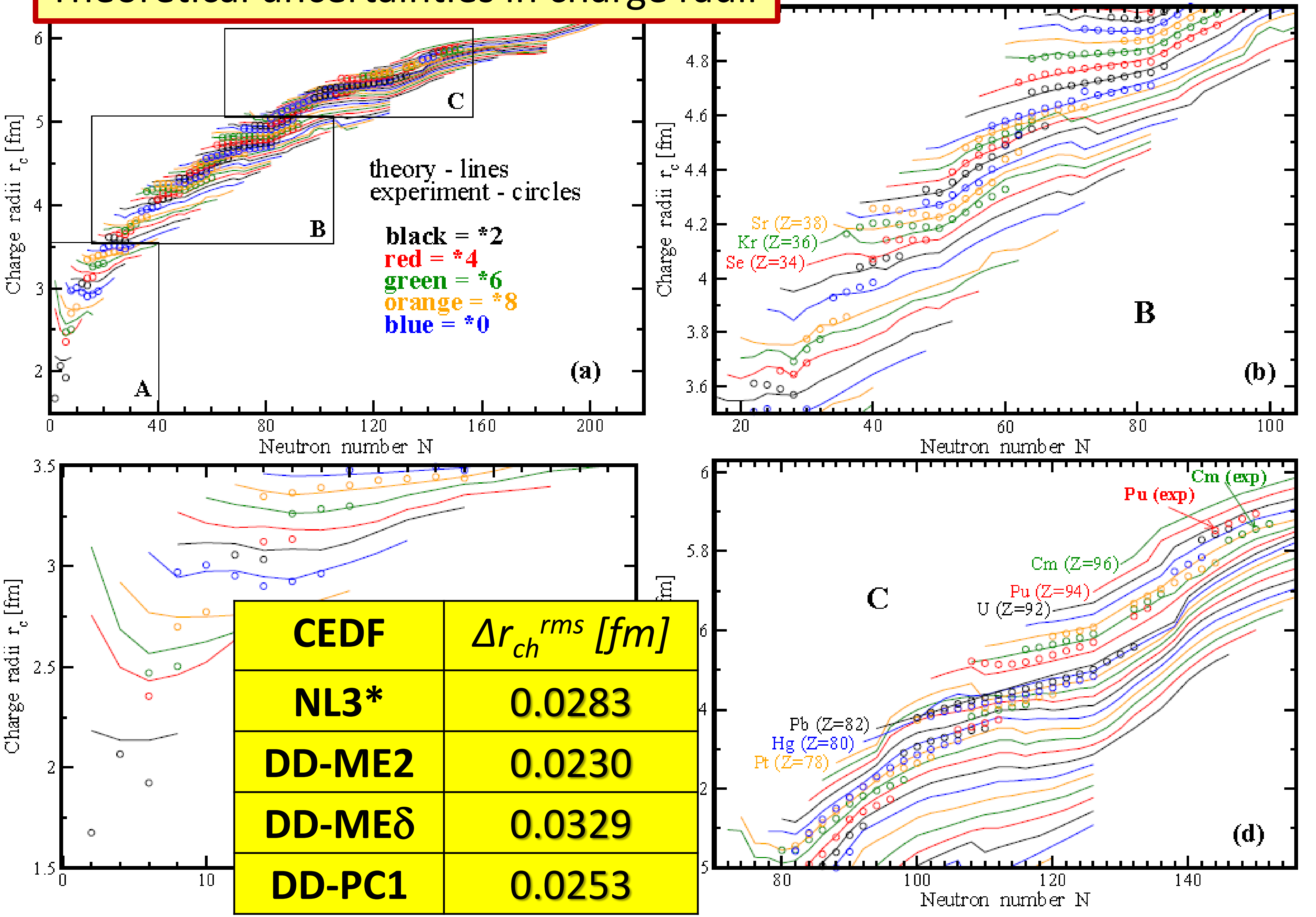

CEDF	Δr_{ch}^{rms} [fm]
NL3*	0.0283
DD-ME2	0.0230
DD-MEδ	0.0329
DD-PC1	0.0253

Neutron skin thicknesses r_{skin} in ^{48}Ca and ^{208}Pb obtained in calculations with the indicated CEDF's.

How large should be neutron skin in ^{208}Pb?

CEDF	$r_{skin}(^{48}\mathrm{Ca})$ [fm]	$r_{skin}(^{208}\mathrm{Pb})$ [fm]
NL3*	0.236	0.288
DD-ME2	0.187	0.193
DD-MEδ	0.177	0.186
DD-PC1	0.198	0.201

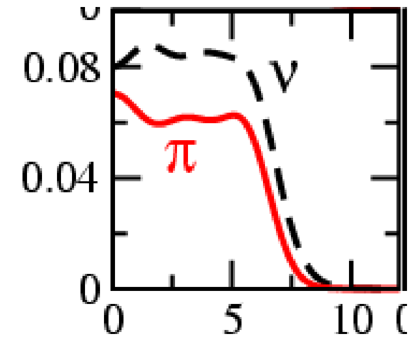

Neutron skin thickness in 208Pb as obtained with different probes

Method	Ref.	Date	ΔR_{pn} (fm)
(p,p) 0.8 GeV	[33]	1980	0.14 ± 0.04
(p,p) 0.65 GeV	[34]	1994	0.20 ± 0.04
$(\alpha,\alpha\prime)$ IVGDR 120 MeV	[13]	1994	0.19 ± 0.09
antiproton absorption	[35]	2001	0.18 ± 0.03
$(\alpha,\alpha\prime)$ IVGDR 200 MeV	[36]	2003	0.12 ± 0.07
pygmy res.	[37]	2007	0.180 ± 0.035
pygmy res.	[38]	2010	0.194 ± 0.024
$(\vec{p},\vec{p}\prime)$	[4]	2011	0.156 ± 0.025
parity viol. (e,e)	[1]	2012	0.33 ± 0.17
AGDR	pres. res.	2013	0.190 ± 0.028

PREX

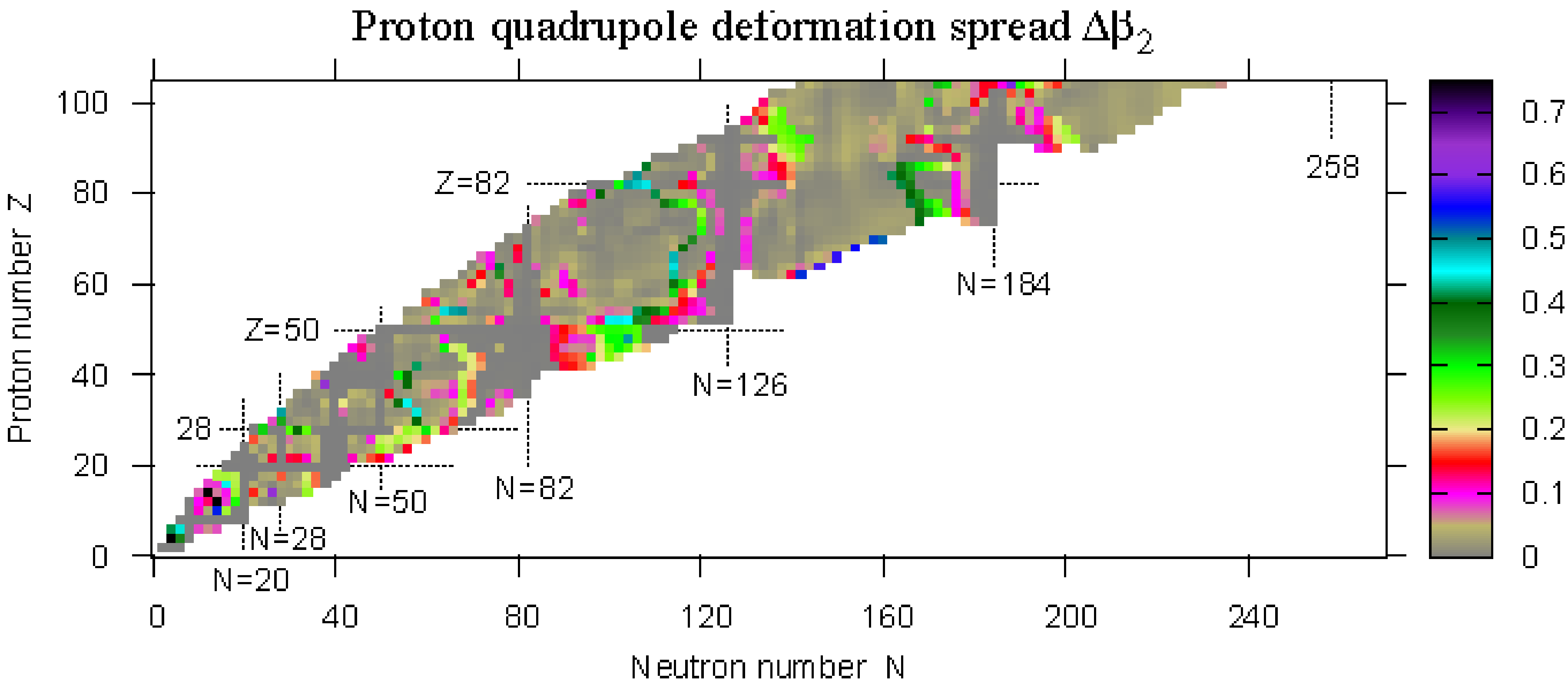

Theoretical uncertainties are most pronounced for transitional nuclei (due to soft potential energy surfaces) and in the regions of transition between prolate and oblate shapes. Details depend of the description of single-particle states

3A. The uncertainties in the predictions and their sources - neutron-drip line

What are the limits of existence of nuclei?

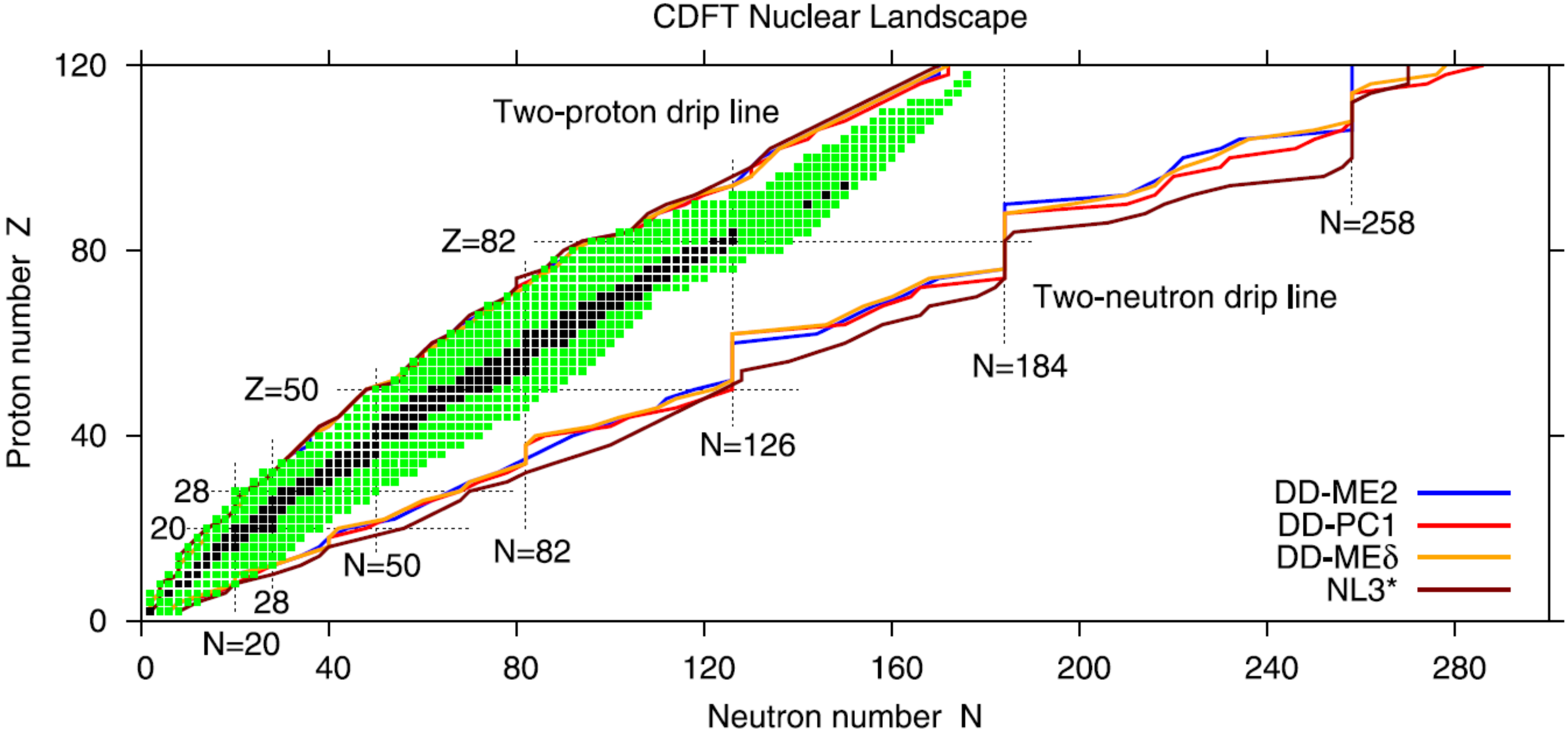

AA, S. Agbemava, D. Ray and P. Ring, PLB 726, 680 (2013)

Skyrme DFT – J.Erler et al, Nature 486, 589 (2012)

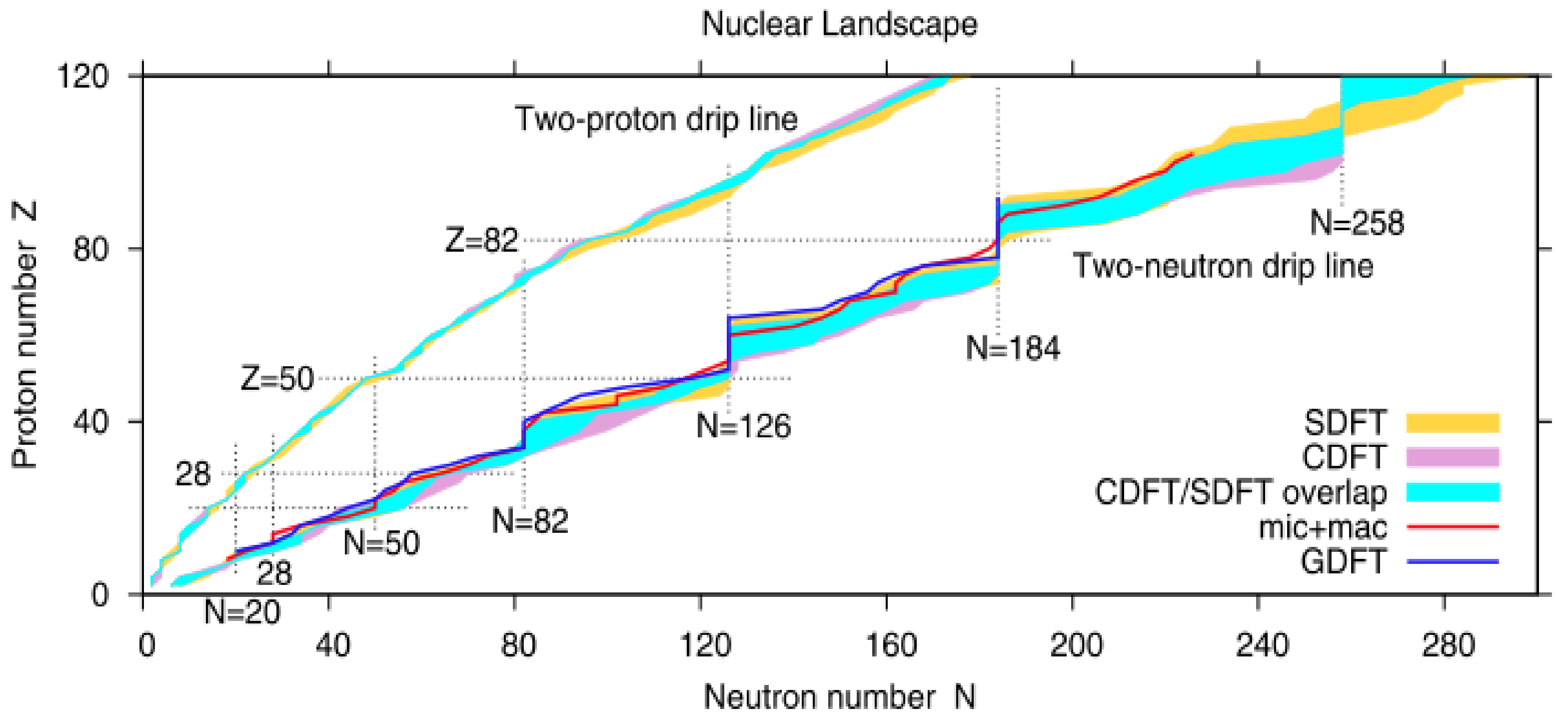

Sources of uncertainties in the prediction of two-neutron drip line

- --- **poorly known isovector properties of energy density functionals** (the position of two-neutron drip line does not correlate with nuclear matter properties of the energy density functional (PLB 726, 680 (2013), PRC 85, 014324 (2014))
- --- **inaccurate description of energies of the single-particle states** (PRC 91, 014324 (2015),
- --- **shallow slope of two-neutron separation energies** (PRC 85, 014324 (2014))

FRIB, RIKEN etc. will help to better understand isovector properties of nuclei, but will not resolve all existing problems. Further theoretical development and refinement of the models are needed.

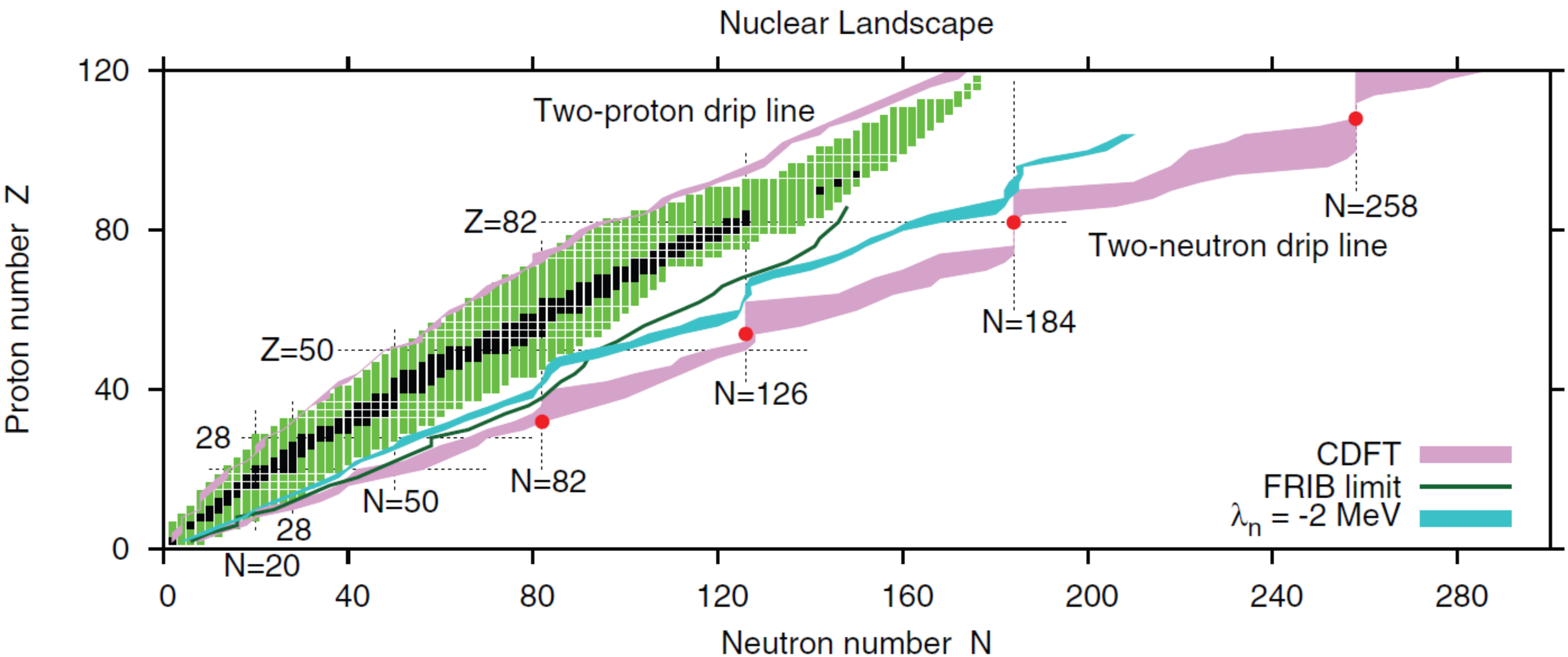

The shell structure still survives in neutron-rich nuclei

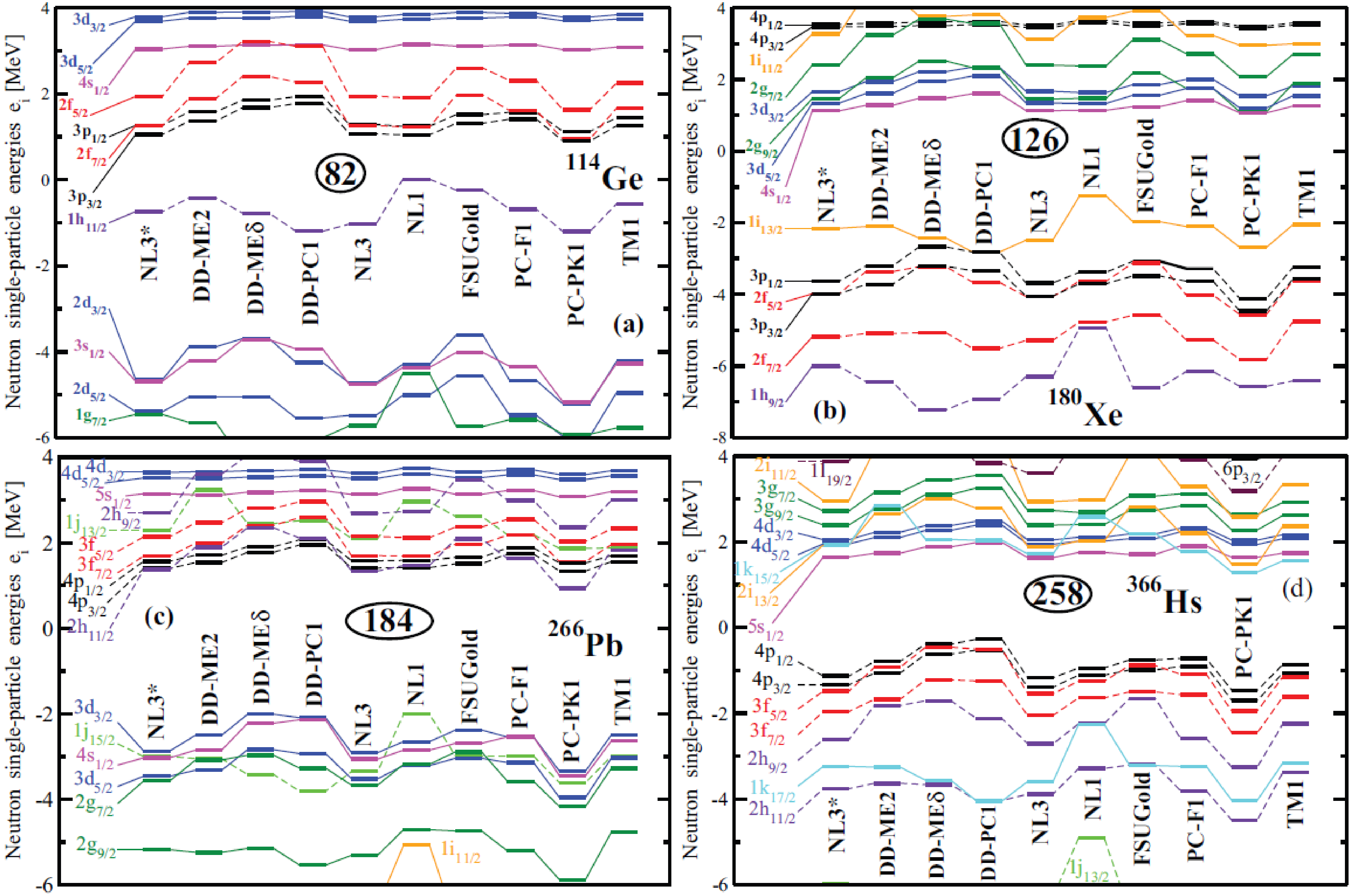

The SHE and two-neutron drip line – the common source of uncertainties (single-particle states)

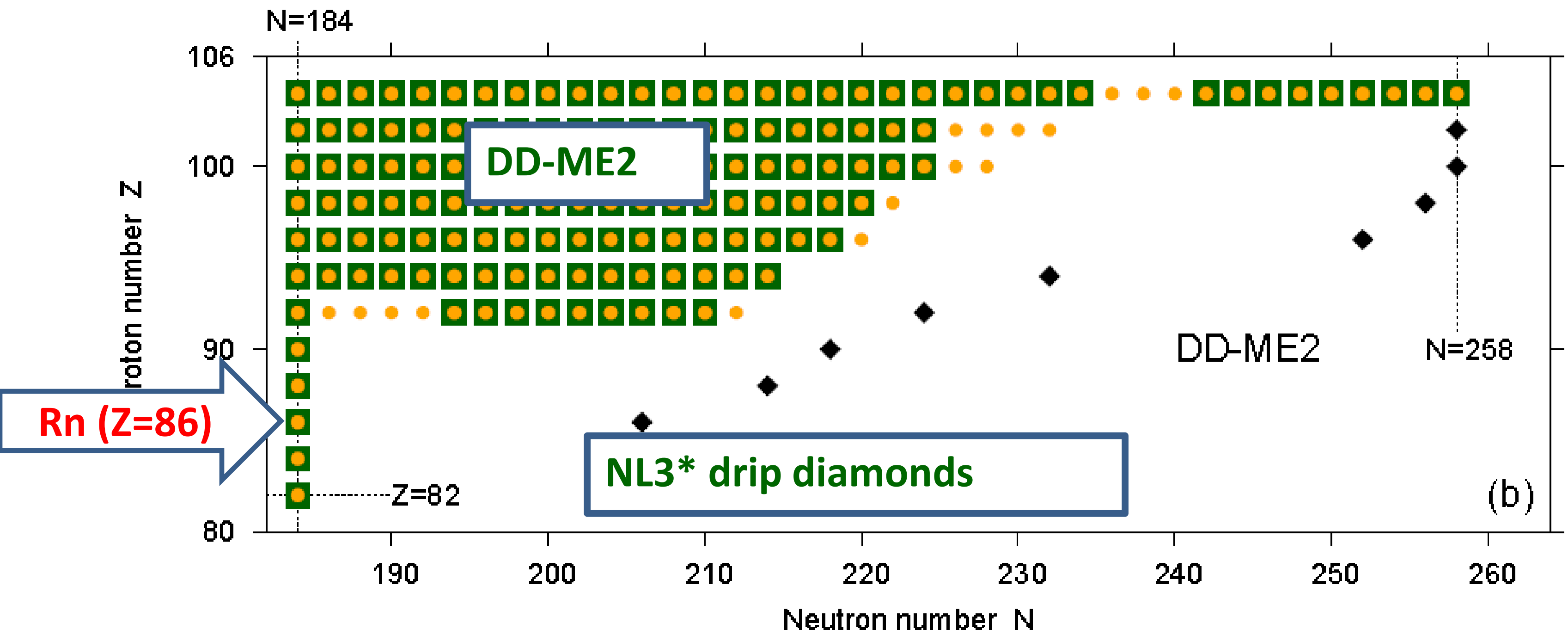

Predictions of two-neutron drip line for DD-Meδ and DD-PC1 are closer to DD-ME2 than to NL3*

The SHE and two-neutron drip line – the common source of uncertainties (single-particle states)

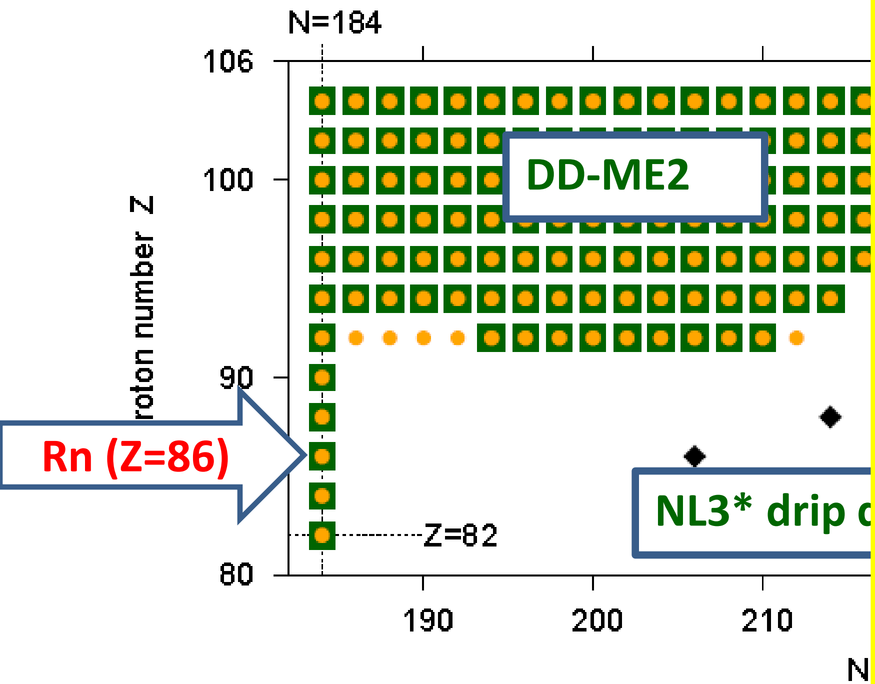

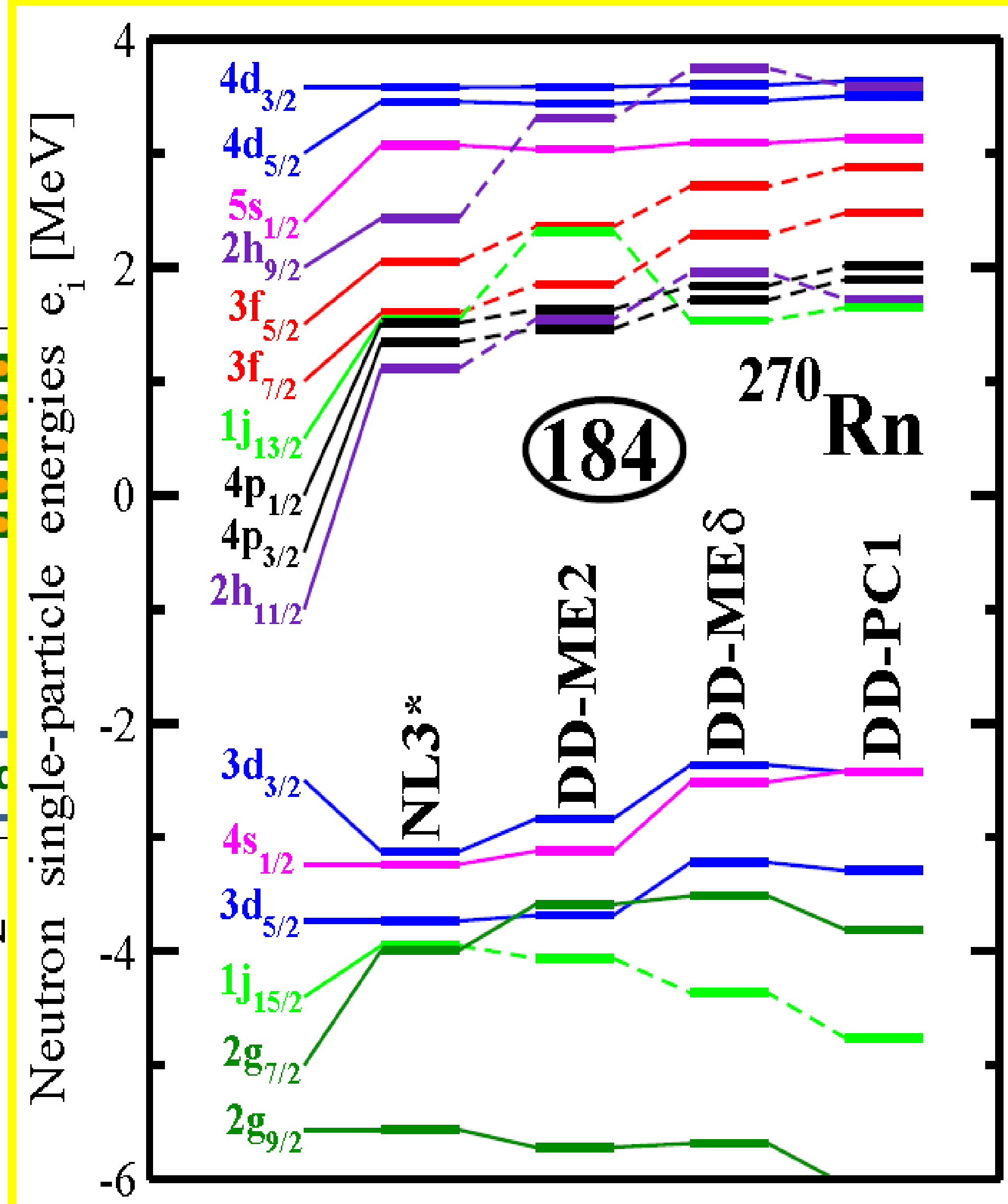

Predictions of two-neutron drip line for DD-Meδ and DD-PC1 are closer to DD-ME2 than to NL3*

Two-neutron drip lines: the impact of uncertainties in single-particle energies

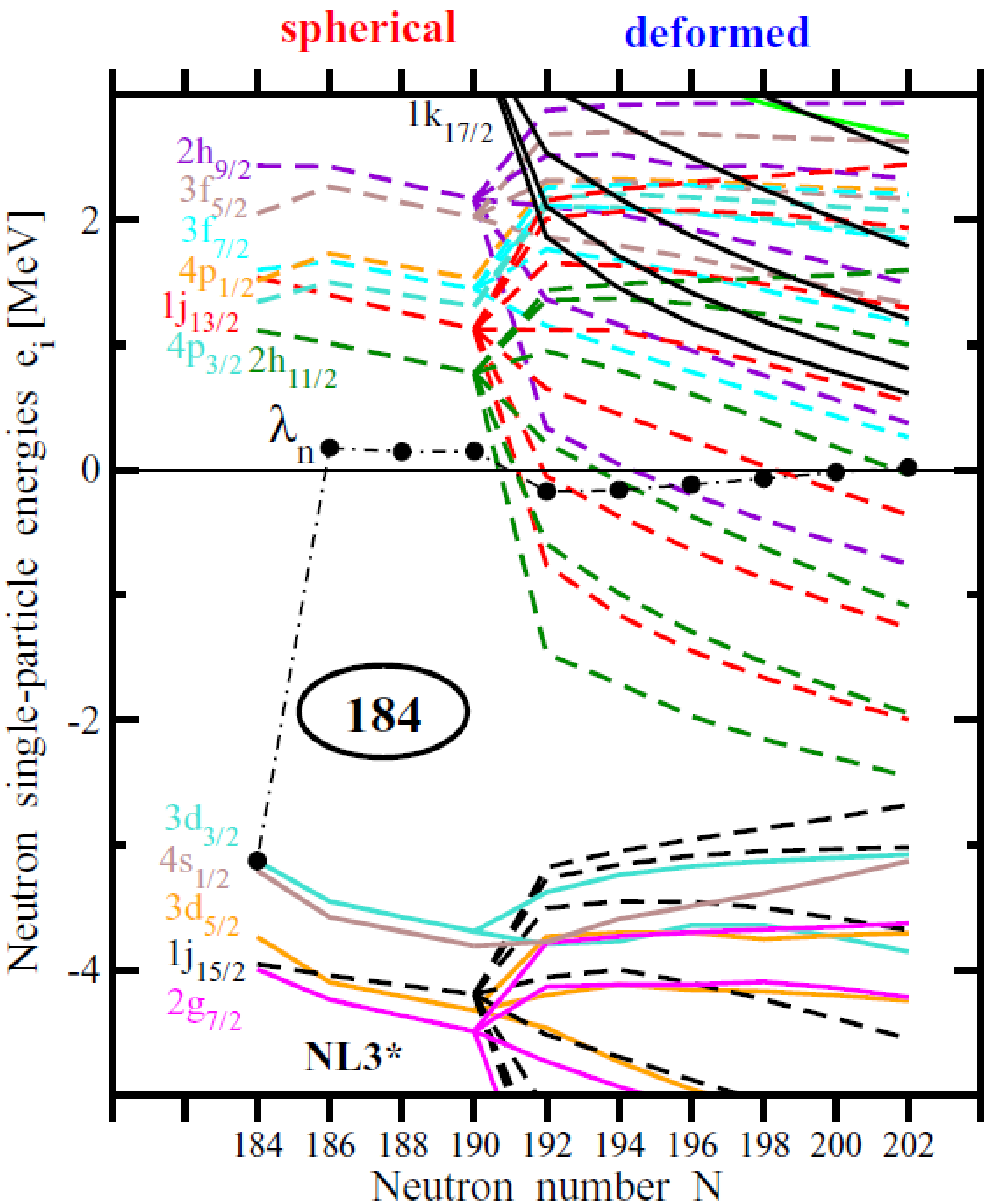

Neutron single-particle energies for the ground-state configurations of the Rn isotopes calculated at their equilibrium deformations as a function of neutron number N. Note that the transition to deformation removes the $2j + 1$ degeneracy of the spherical orbitals.

calculational scheme "B"

Reducing uncertainties for two-neutron drip line

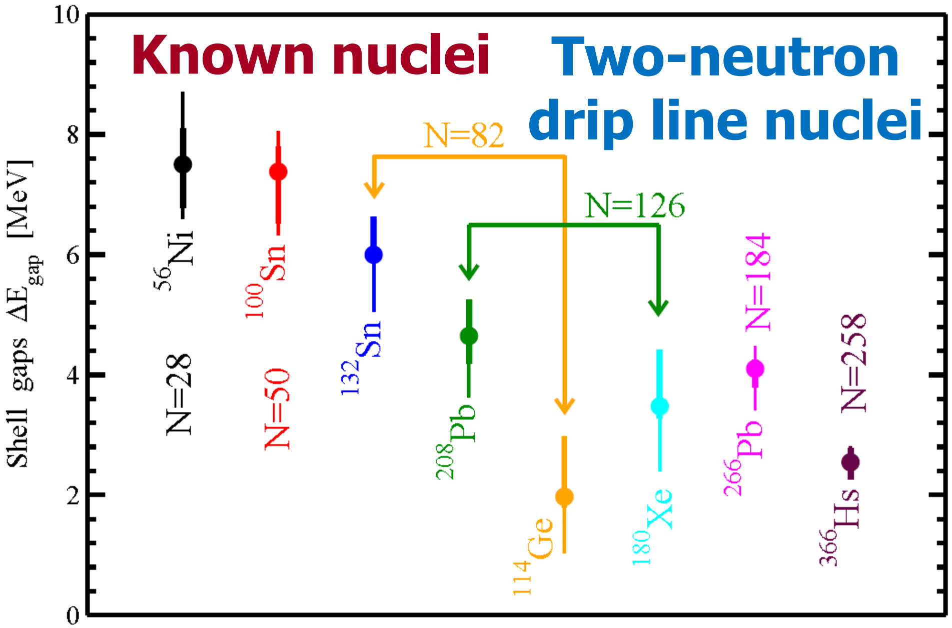

Thin lines – 10 CEDF, thick – 4 CEDF

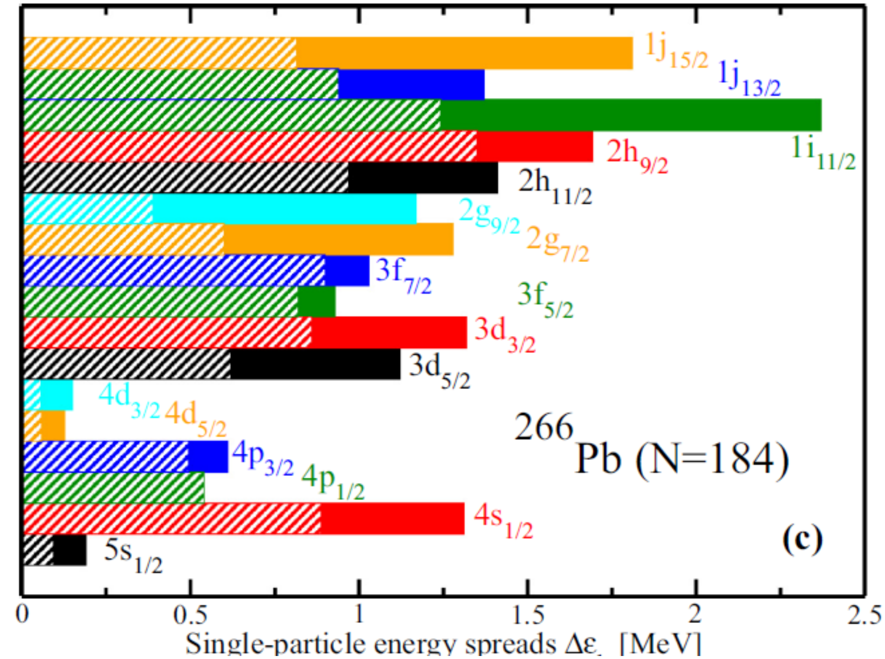

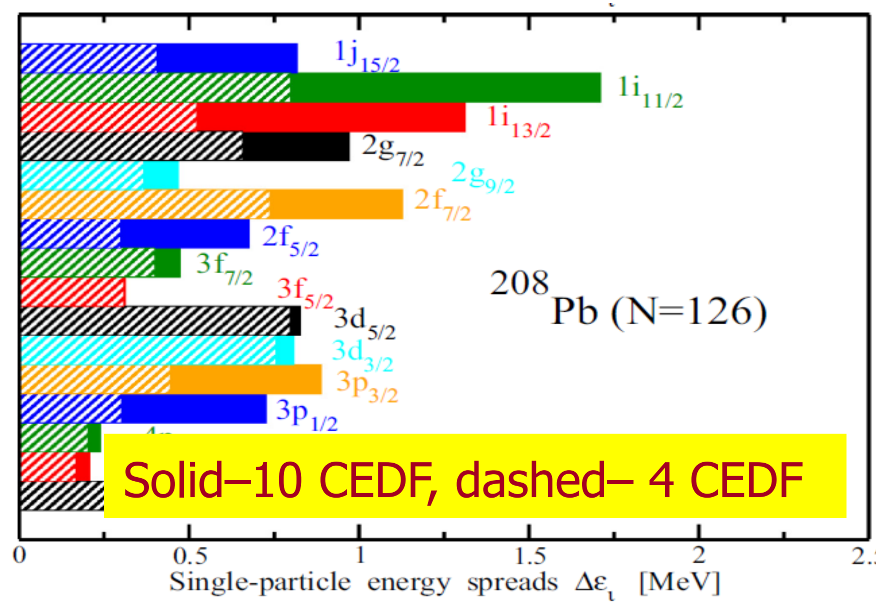

Solid–10 CEDF, dashed– 4 CEDF

3B. The uncertainties in the predictions and their sources

- superheavy nuclei

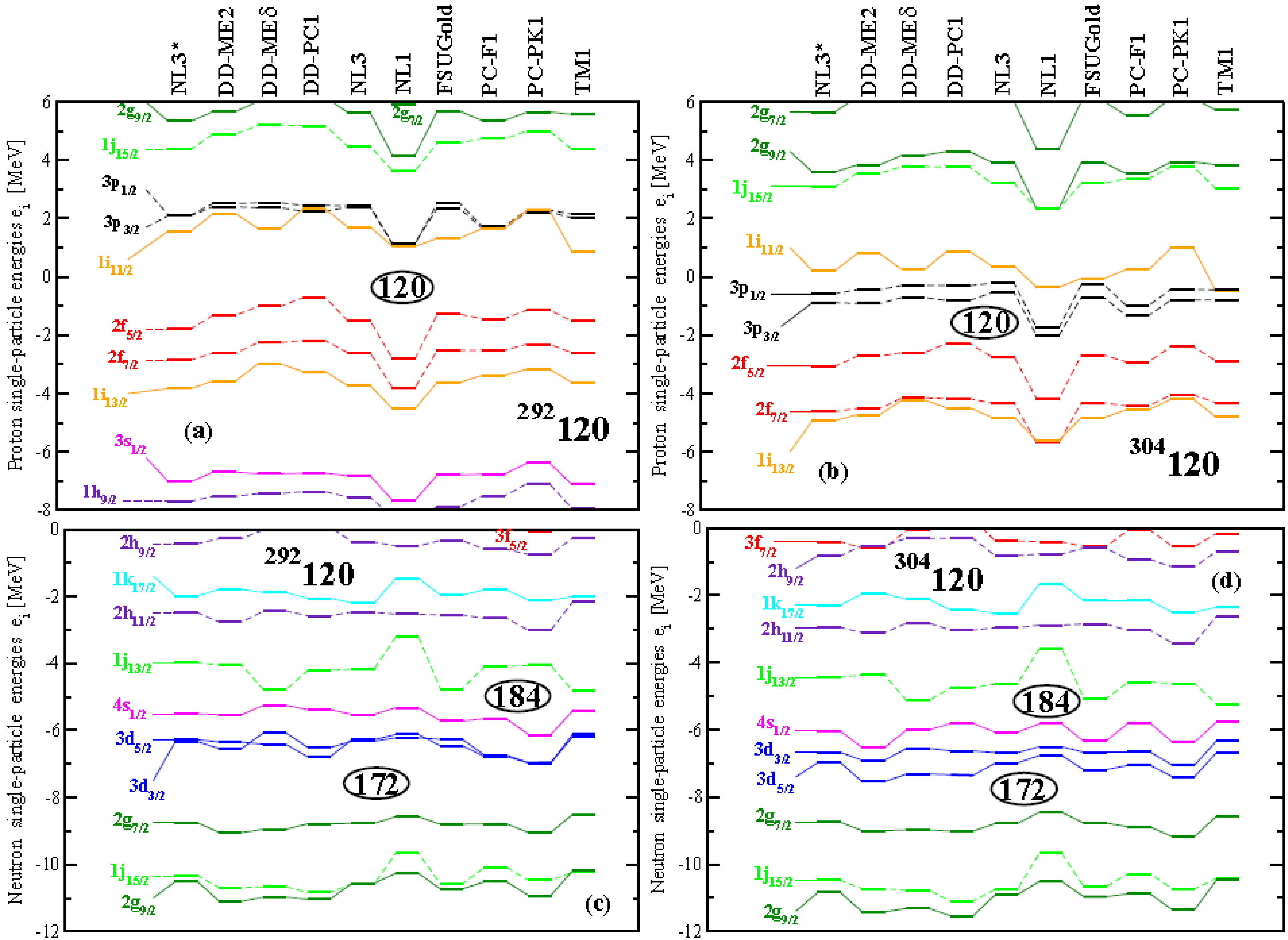

NL3*
DD-ME2
DD-MEδ
DD-PC1
NL3
NL1
FSUGold
PC-F1
PC-PK1
TM1
Proton single-particle energies e_i [MeV]
Neutron single-particle energies e_i [MeV]
(a)
$^{292}120$
120
$2g_{9/2}$
$2g_{7/2}$
$1j_{15/2}$
$3p_{1/2}$
$3p_{3/2}$
$1i_{11/2}$
$2f_{5/2}$
$2f_{7/2}$
$1i_{13/2}$
$3s_{1/2}$
$1h_{9/2}$
(b)
$^{304}120$
120
$2g_{7/2}$
$2g_{9/2}$
$1j_{15/2}$
$1i_{11/2}$
$3p_{1/2}$
$3p_{3/2}$
$2f_{5/2}$
$2f_{7/2}$
$1i_{13/2}$
(c)
$^{292}120$
184
172
$2h_{9/2}$
$3f_{5/2}$
$1k_{17/2}$
$2h_{11/2}$
$1j_{13/2}$
$4s_{1/2}$
$3d_{5/2}$
$3d_{3/2}$
$2g_{7/2}$
$1j_{15/2}$
$2g_{9/2}$
(d)
$^{304}120$
184
172
$3f_{7/2}$
$2h_{9/2}$
$1k_{17/2}$
$2h_{11/2}$
$1j_{13/2}$
$4s_{1/2}$
$3d_{3/2}$
$3d_{5/2}$
$2g_{7/2}$
$1j_{15/2}$
$2g_{9/2}$

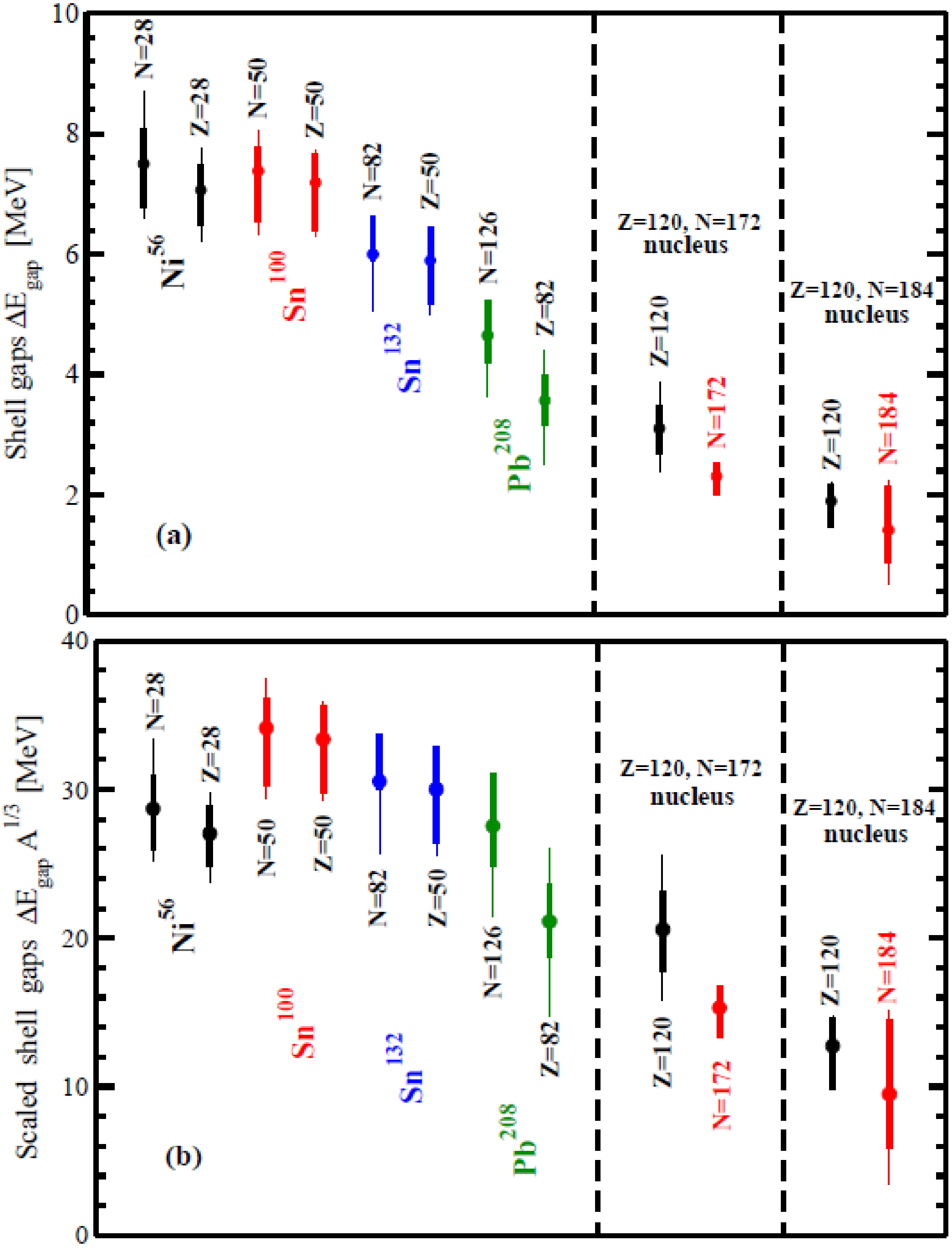

Theoretical uncertainties in the prediction of the sizes of shell gaps.

Thin lines – all 10 CEDF's, thick – 4 CEDF (NL3*,DD-ME2, DD-MEδ,DD-PC1)

Mass dependence of single-particle level density ($\sim A^{1/3}$) is taken into account

Deformation effects on shell structure

→ Very important – deformed results differ substantially from spherical ones

Unusual feature: oblate shapes above the shell closures

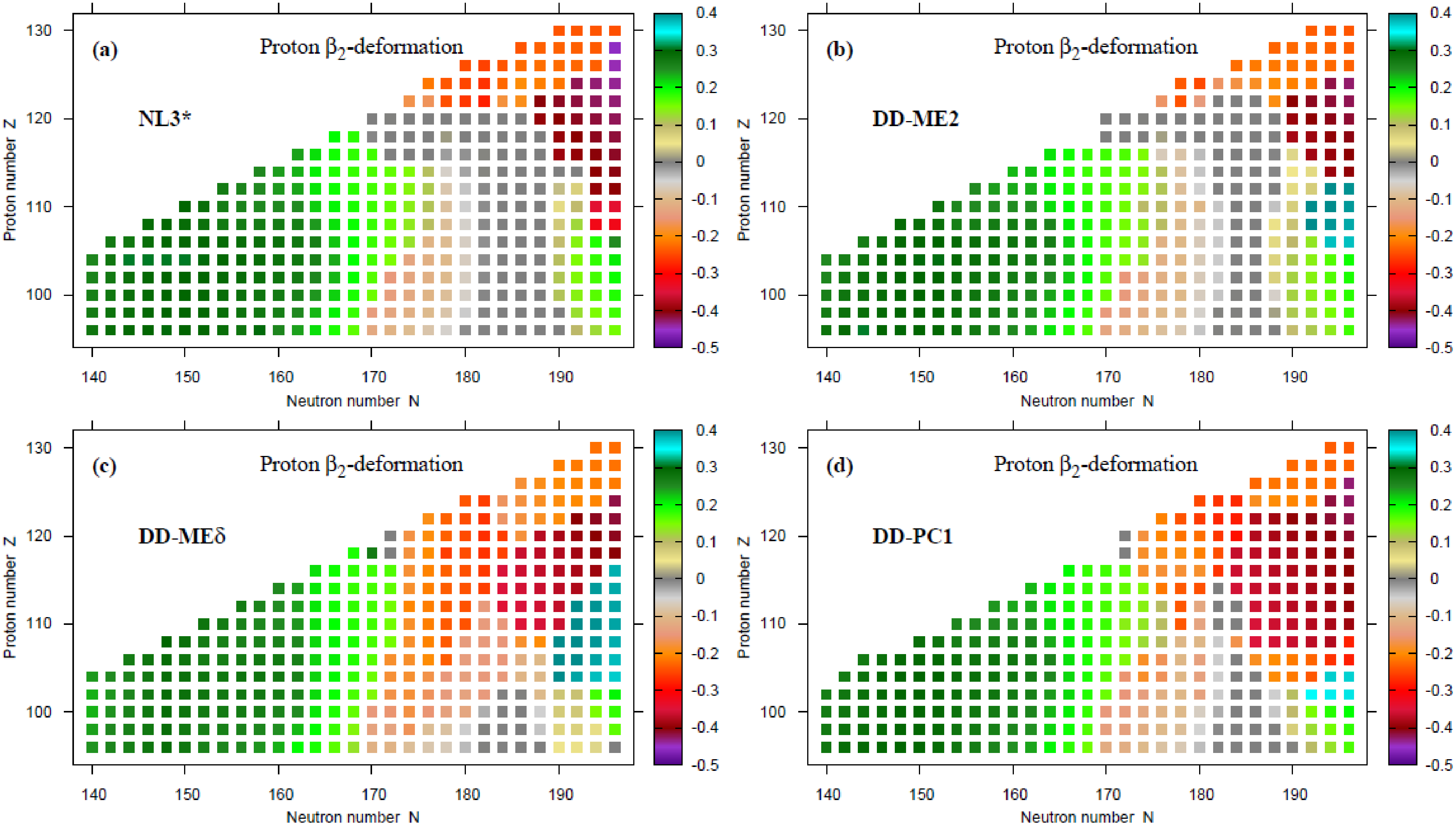

Results for PC-PK1 are very similar to the ones with NL3*

The spreads (theoretical uncertainties) in the deformations

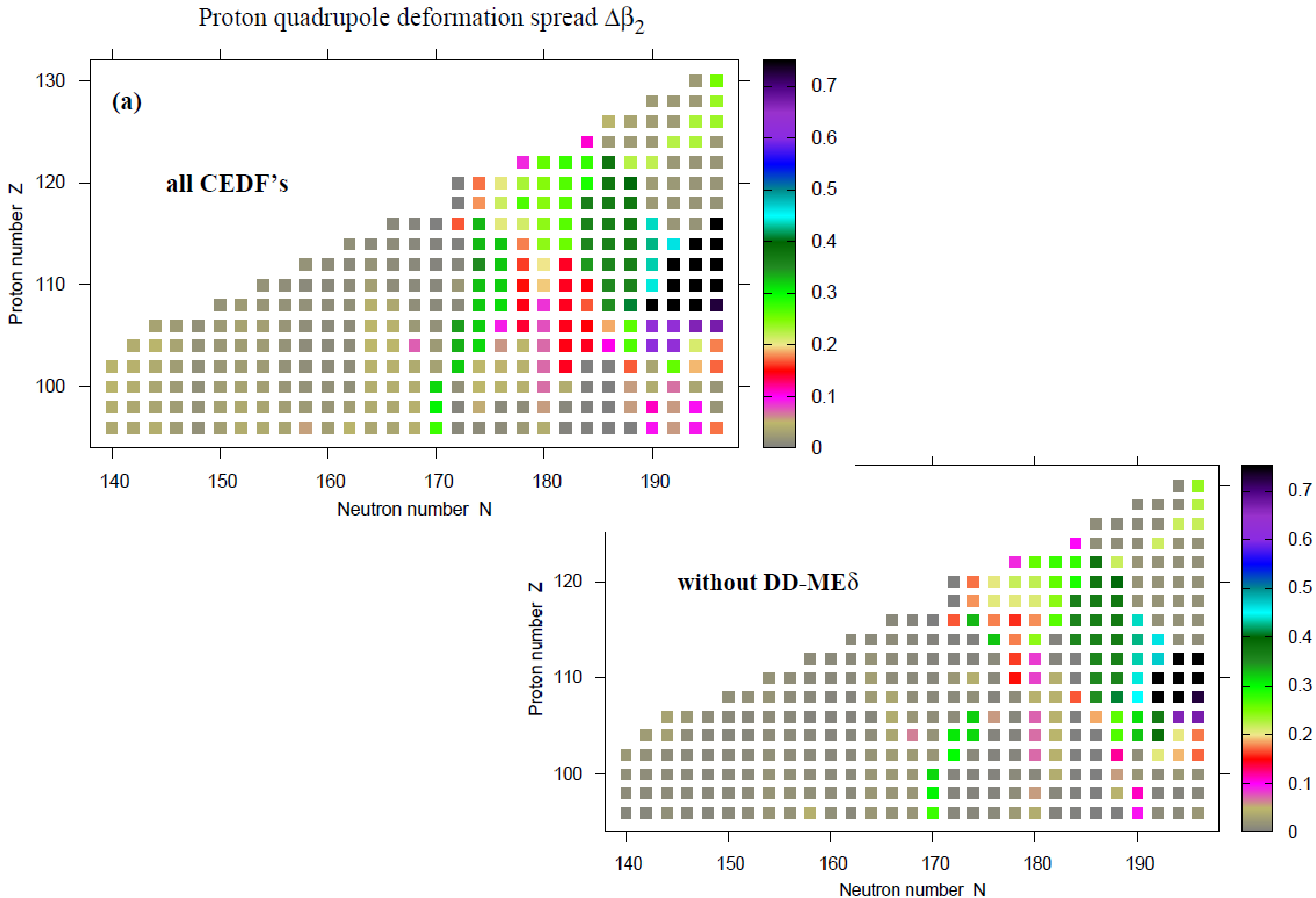

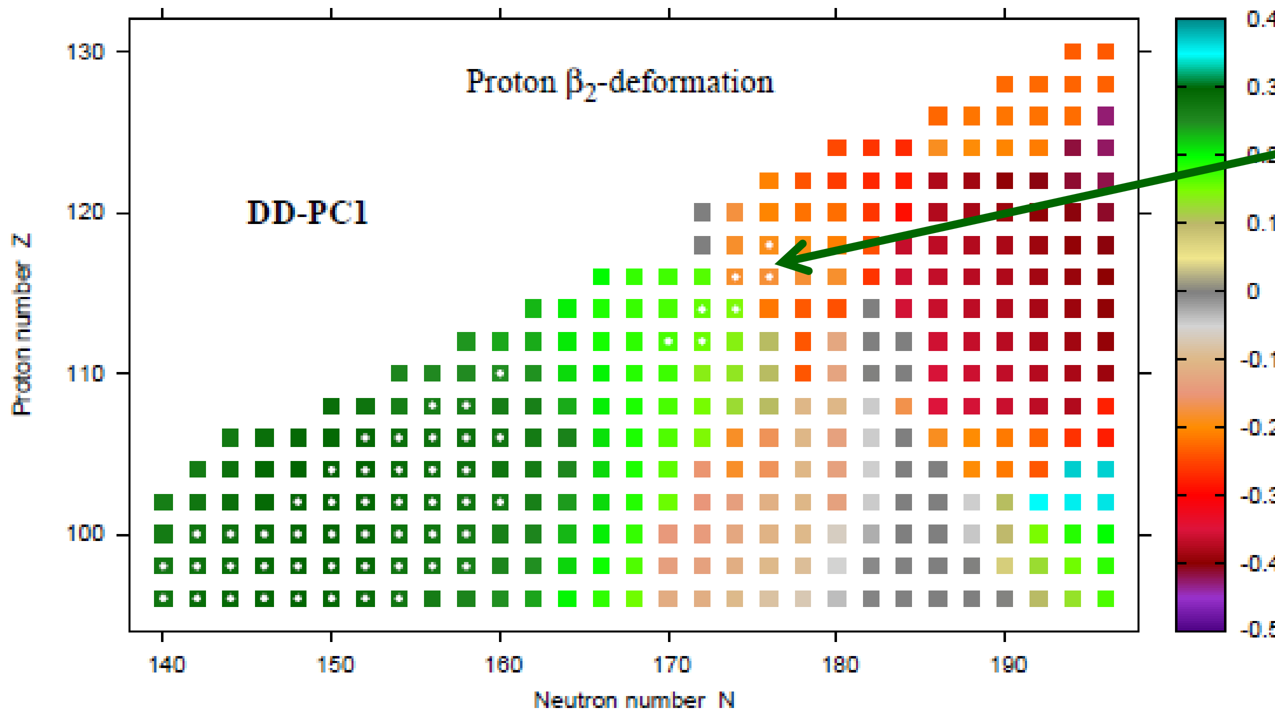

DD-PC1:
Experimental
Z=116, 118
nuclei are oblate

PC-PK1:
Experimental
Z=118 nucleus
is spherical

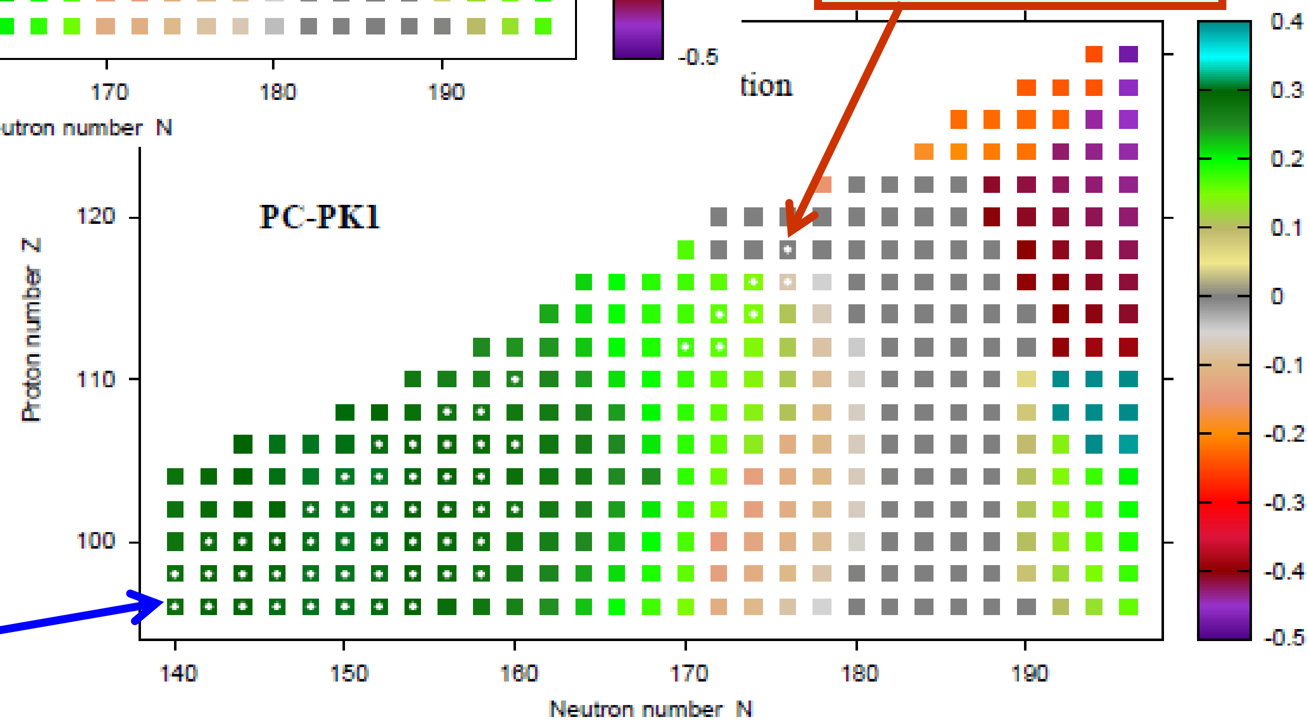

Other experimental
SHE are prolate

Open circles –
experimentally
observed nuclei

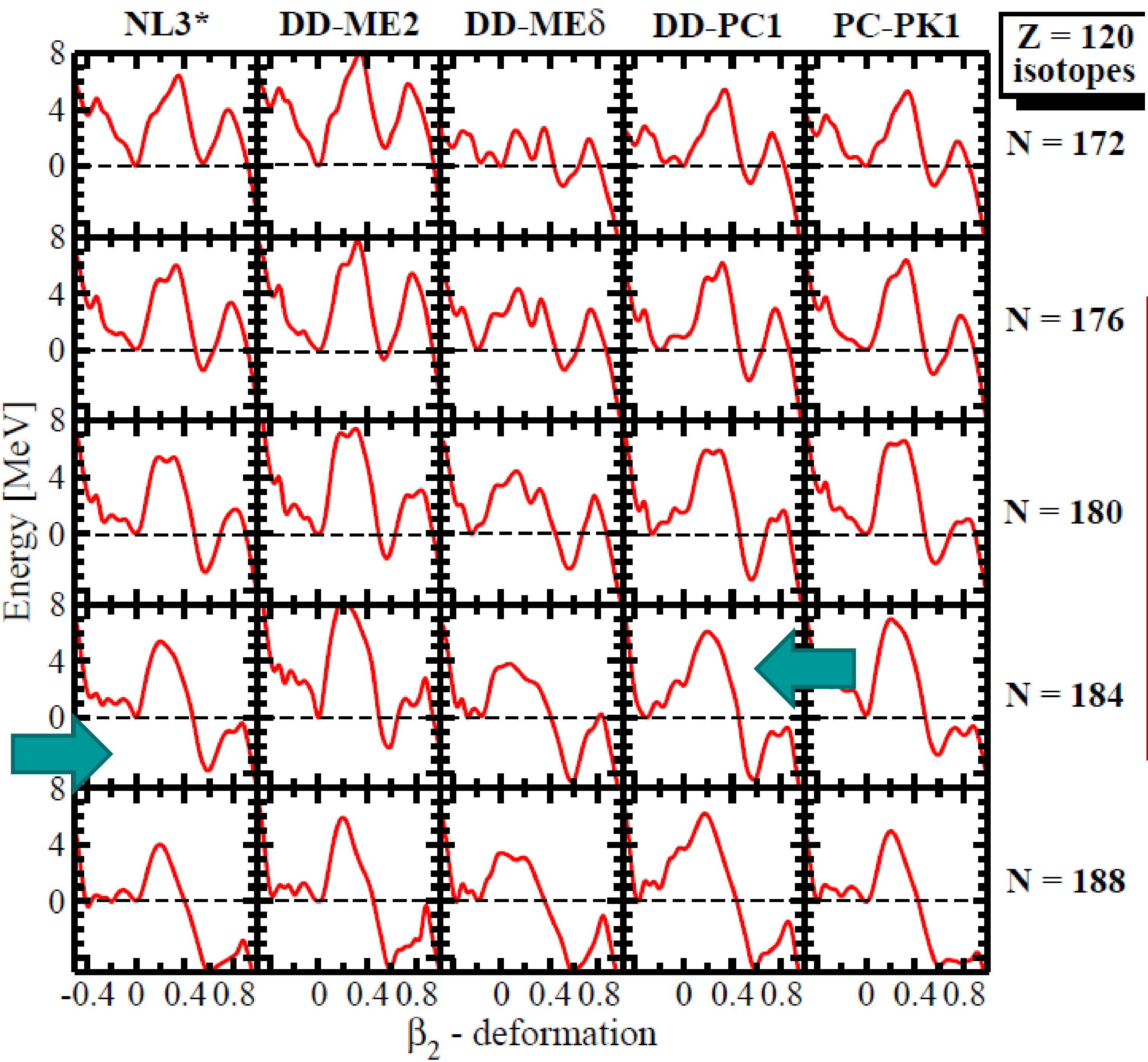

Potential energy surfaces in axially symmetric RHB calculations with separable pairing

The source of oblate shapes – the low density of s-p states

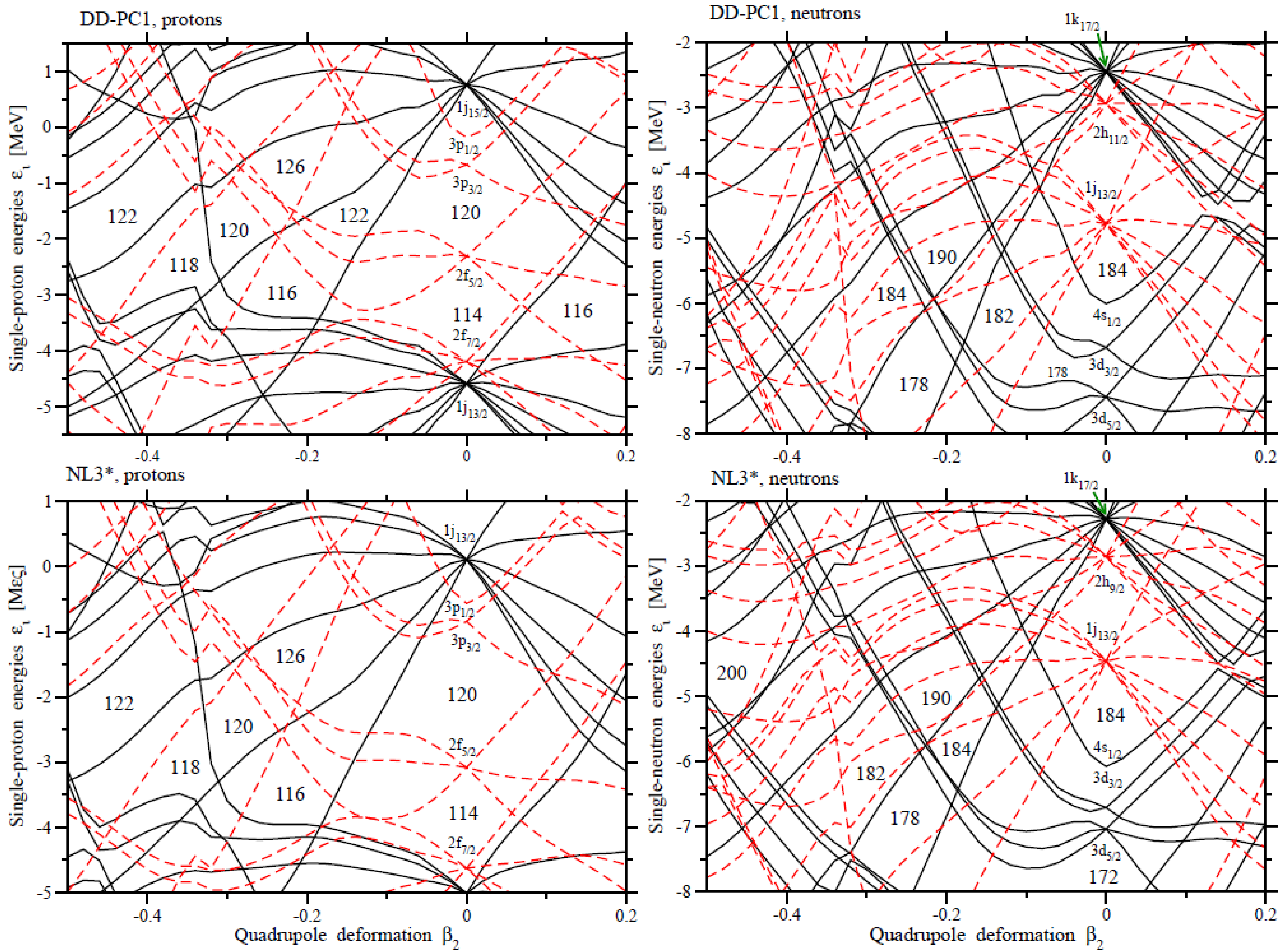

Accuracy of the description of experimental data in Z>94 nuclei

CEDF	ΔE_{rms} [MeV]	$\Delta(S_{2n})_{rms}$ [MeV]	$\Delta(S_{2p})_{rms}$ [MeV]	$\Delta(Q_\alpha)_{rms}$ [MeV]
1	2	3	4	5
NL3*	3.02/3.39	0.71/0.68	1.33/1.34	0.68/0.75
DD-ME2	1.39/1.40	0.45/0.54	0.85/0.90	0.51/0.65
DD-MEδ	2.52/2.45	0.60/0.51	0.45/0.48	0.39/0.51
DD-PC1	**0.59/0.74**	0.30/0.32	0.41/0.42	0.36/0.47
PC-PK1	2.82/2.63	**0.25/0.23**	**0.36/0.33**	**0.32/0.38**

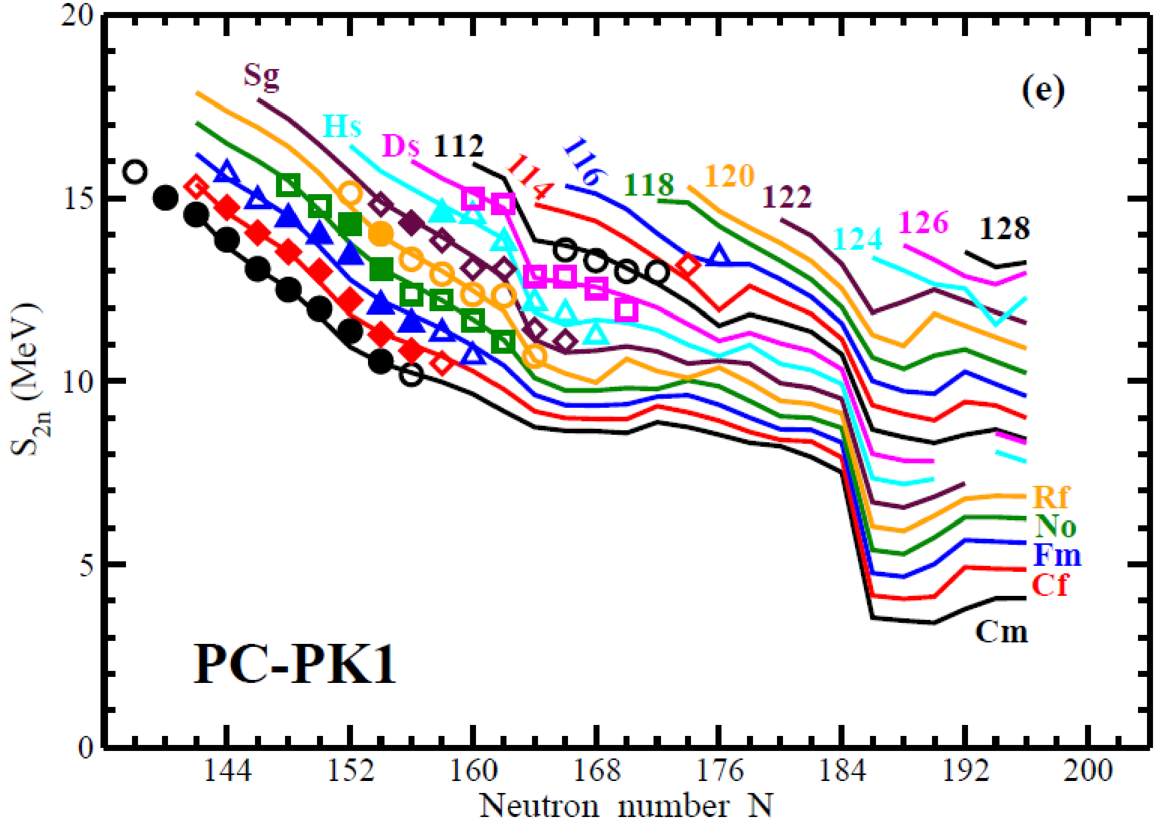

With exception of the DD-MEδ, the deformed N=162 gap is well reproduced in all CEDF's

The Q_α-values

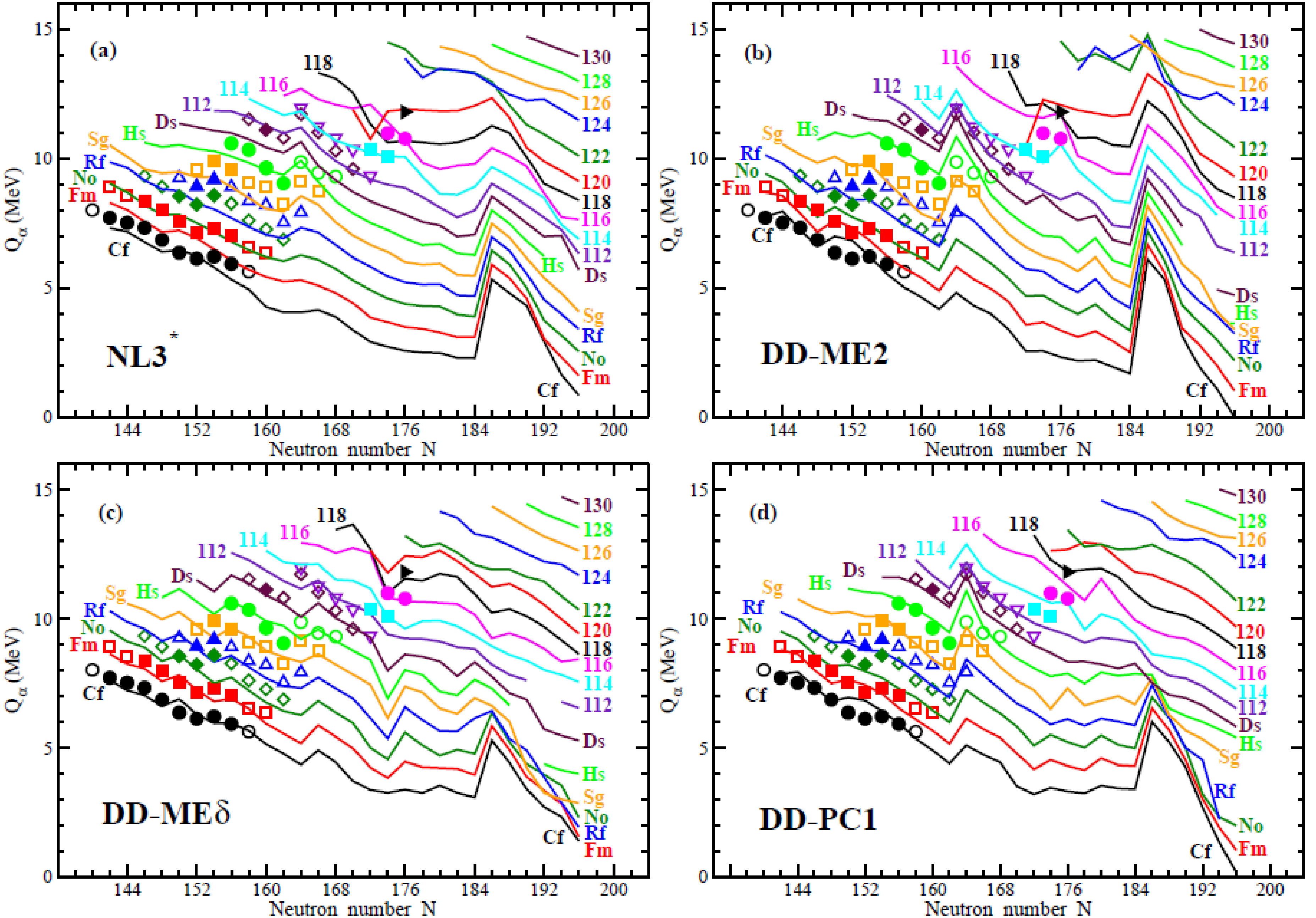

Fission barriers: theory versus experiment [state-of-the-art]

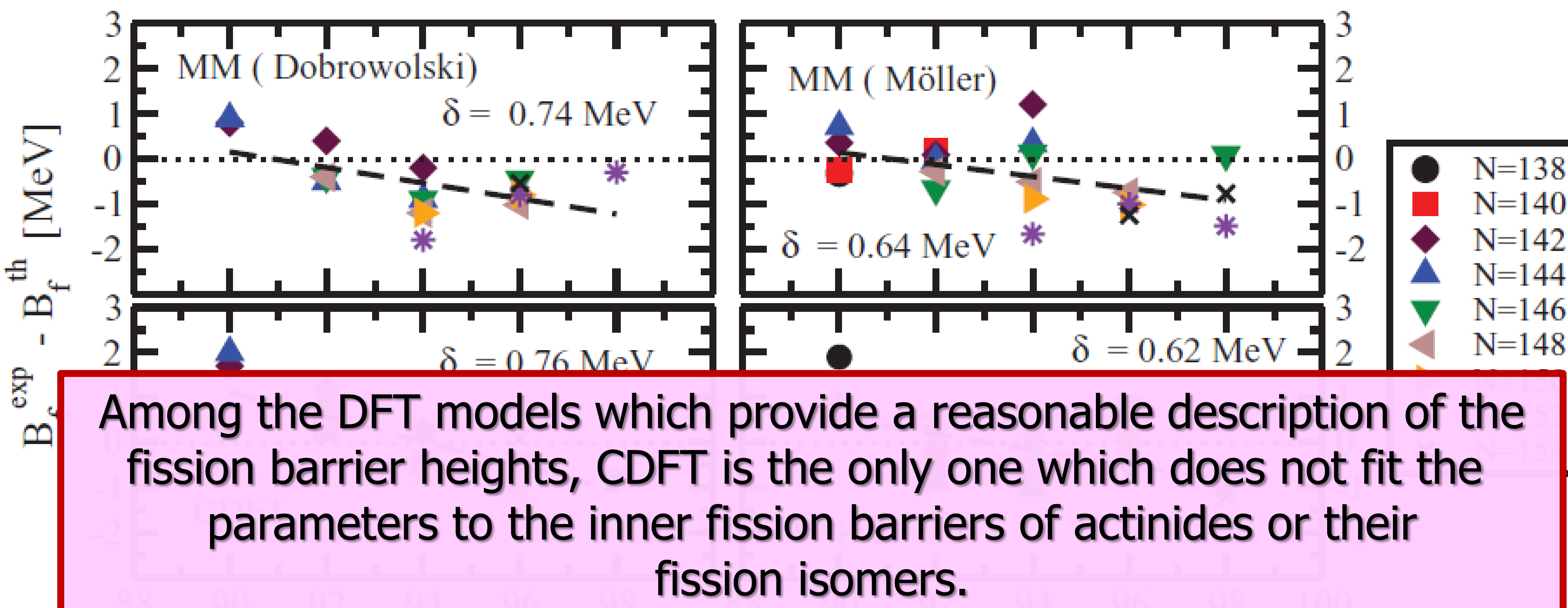

Among the DFT models which provide a reasonable description of the fission barrier heights, CDFT is the only one which does not fit the parameters to the inner fission barriers of actinides or their fission isomers.
Note also that liquid drop parameters of many mic+mac calculations are fitted to experimental fission barriers.

Mac+mic, LSD model
A.Dobrowolski et al,
PRC 75, 024613 (2007)

Mac+mic, FRDM model
P. Moller et al,
PRC 79, 064304 (2009)

Gogny DFT,
J.-P. Delaroche et al,
NPA 771, 103 (2006).

CDFT : actinides H. Abusara, AA and P. Ring, PRC 82, 044303 (2010)
superheavies: H. Abusara, AA and P. Ring, PRC 85, 024314 (2012)

The heights of inner fission barriers in superheavy nuclei

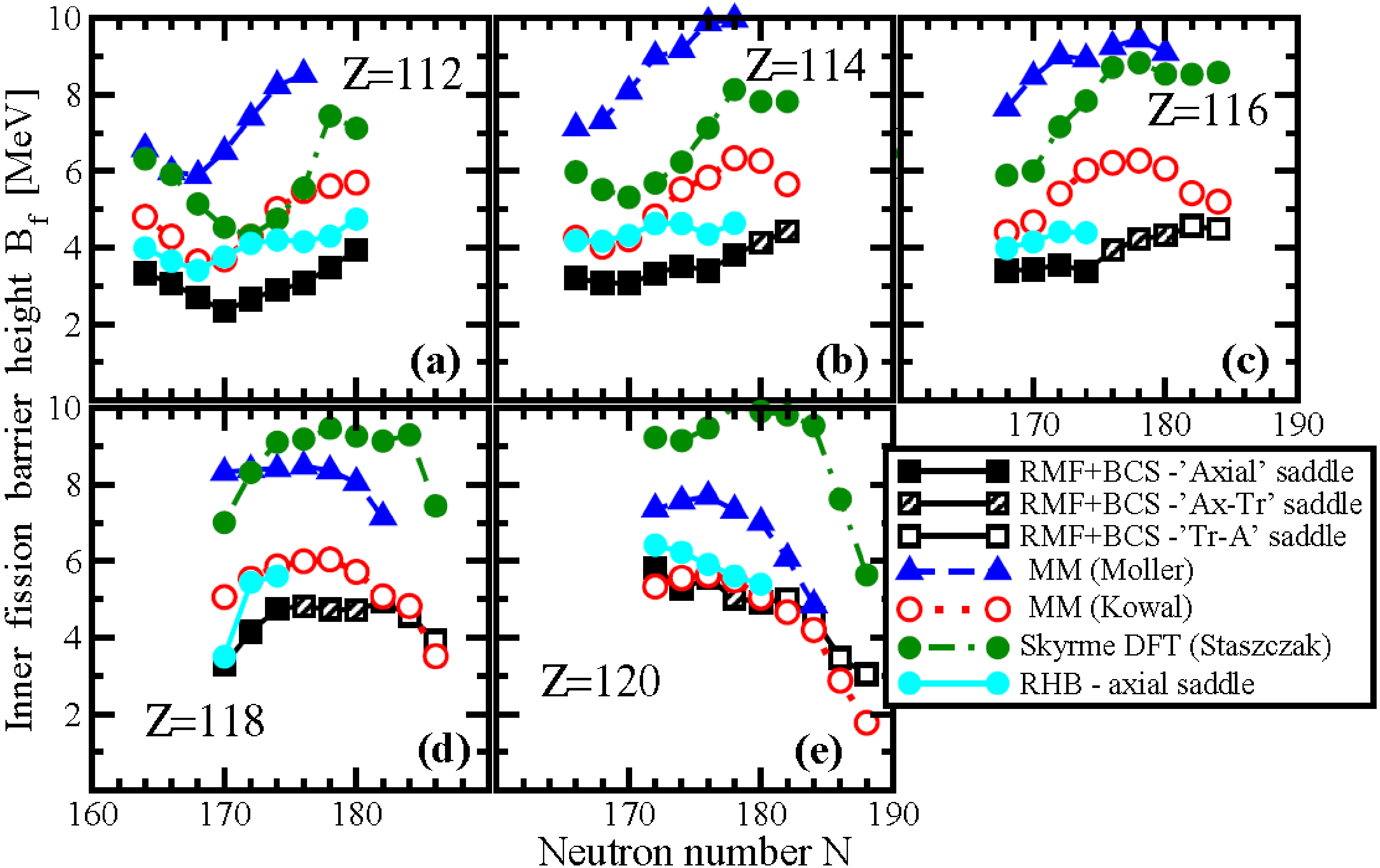

AA, S. Agbemava, Acta Physica Polonica, 46, 405 (2015)

A. Staszczak et al, PRC 87, 024320 (2013) – Skyrme SkM*
M. Kowal et al, PRC 82, 014303 (2010) – WS pot. + Yukawa exponent. model
P. Moller et al, PRC 79, 064304 (2009) – folded Yukawa pot. + FRDM model

The spreads (theoretical uncertainties) in the heights of inner fission barriers in superheavy nuclei

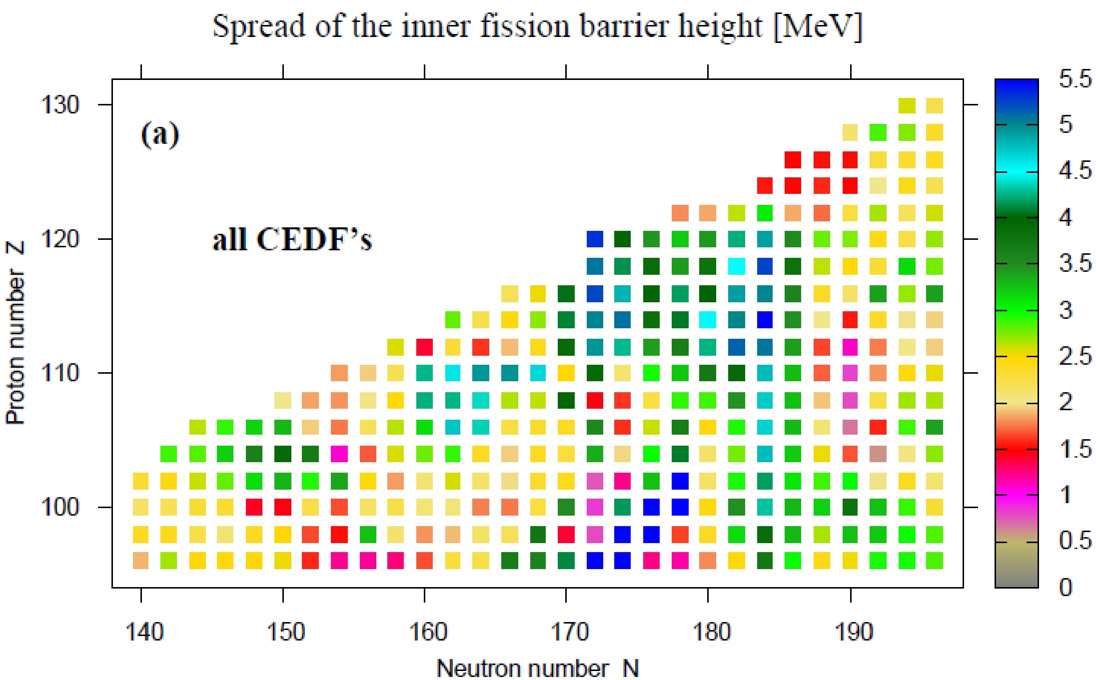

Axial RHB calculations

Benchmarking of fission barriers in actinides (done for NL3*, DD-PC1 and PC-PK1) reduces theoretical uncertainties and makes the description of fission barriers more predictive

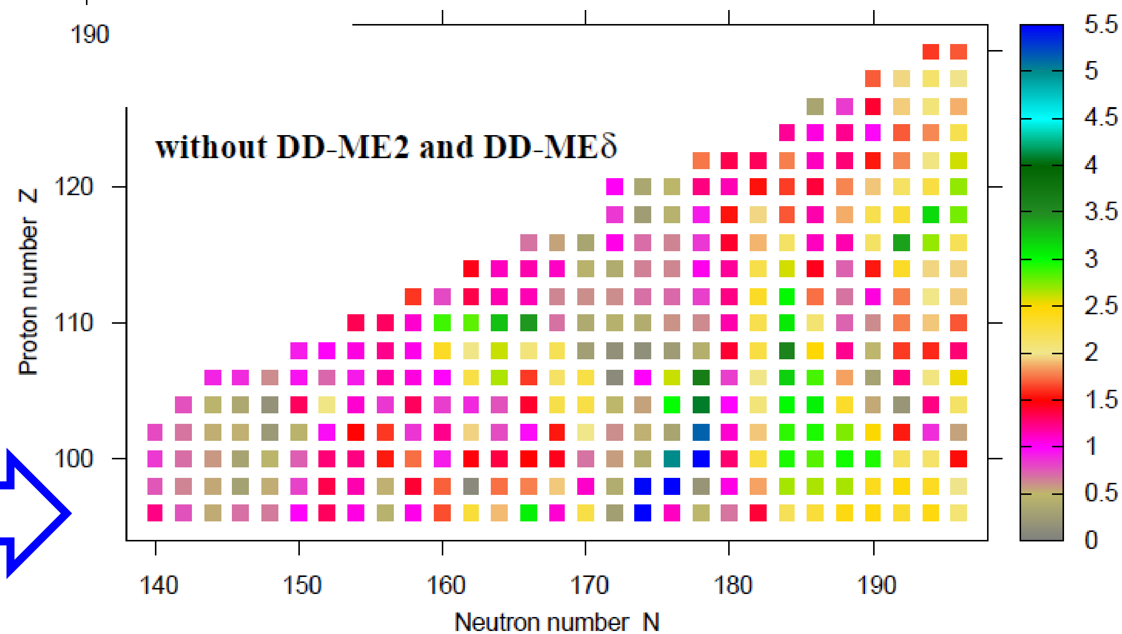

Fission recycling in dynamically ejected matter of neutron star mergers.

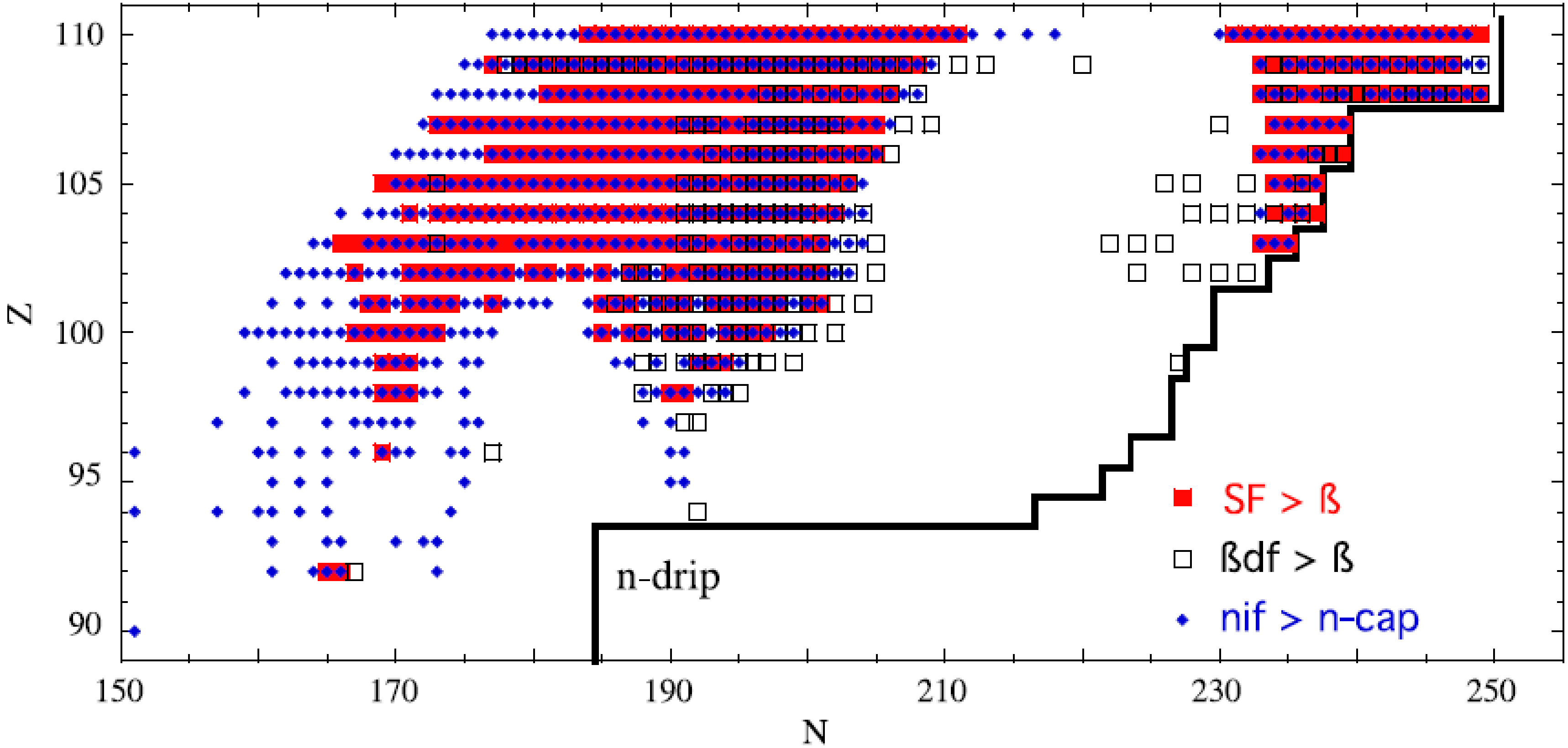

Dominant fission regions in the (N,Z) plane. Nuclei for which spontaneous fission is estimated to be faster than β-decays are shown by full squares, those for which β-delayed fission is faster than β-decays by open circles, and those for which neutron-induced fission is faster than radiative neutron capture at $T=10^9$ by diamonds.

From S. Goriely et al, AJL 738, L32 (2011)

Single-particle energies: how to improve their description?

E. Litvinova, AA, PRC 84, 014305 (2011)

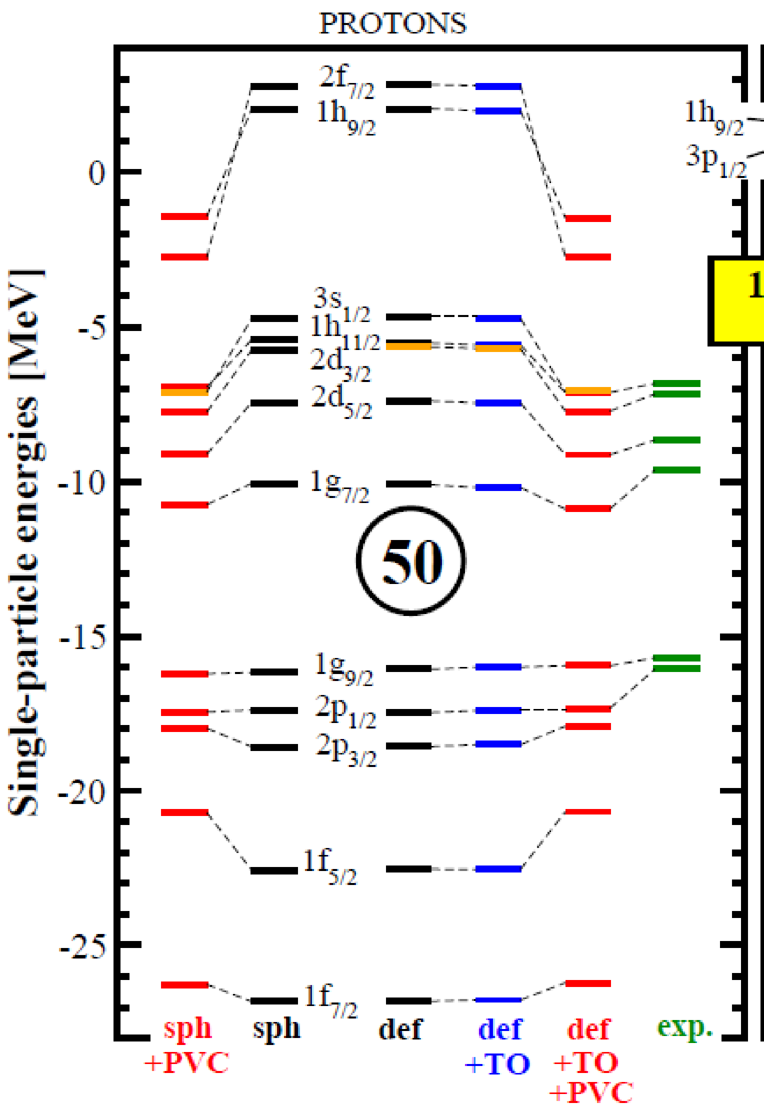

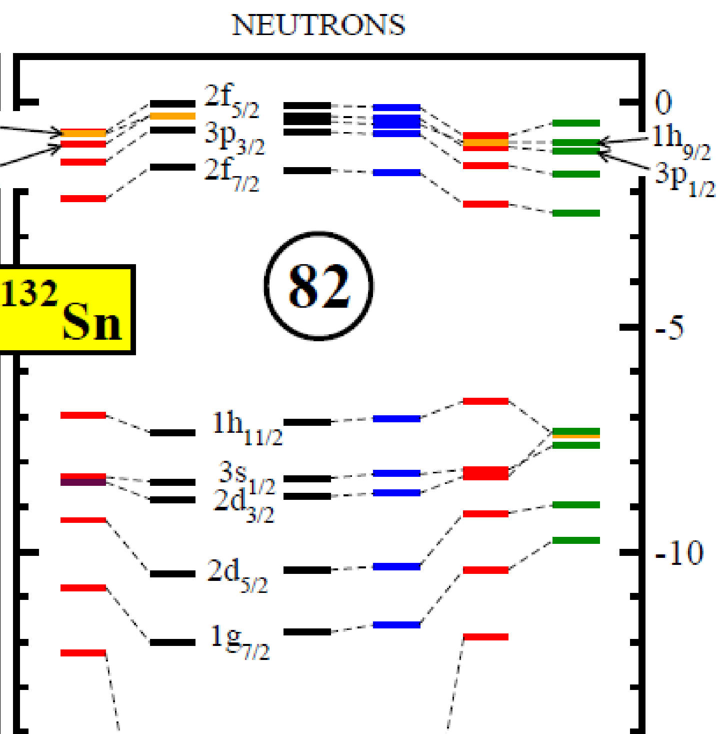

NL3* parametrization

particle-vibration coupling
+ TO, TE polarization effects

TABLE I: Average deviations per state $\Delta\epsilon$ between calculated and experimental energies of the single-particle states for a proton (neutron) subsystem of a given nucleus. The results

Nucleus/subsystem	$\Delta\epsilon_{def+TO}$ [MeV]	$\Delta\epsilon_{def+TO+PVC}$ [MeV]
^{56}Ni/proton	0.76	0.77
^{56}Ni/neutron	0.89	0.71
^{132}Sn/proton	1.02	0.68
^{132}Sn/neutron	0.89	0.39
^{208}Pb/proton	1.53	0.84
^{208}Pb/neutron	1.00	0.47

Statistical distribution of deviations of the energies of one-quasiparticle states from experiment

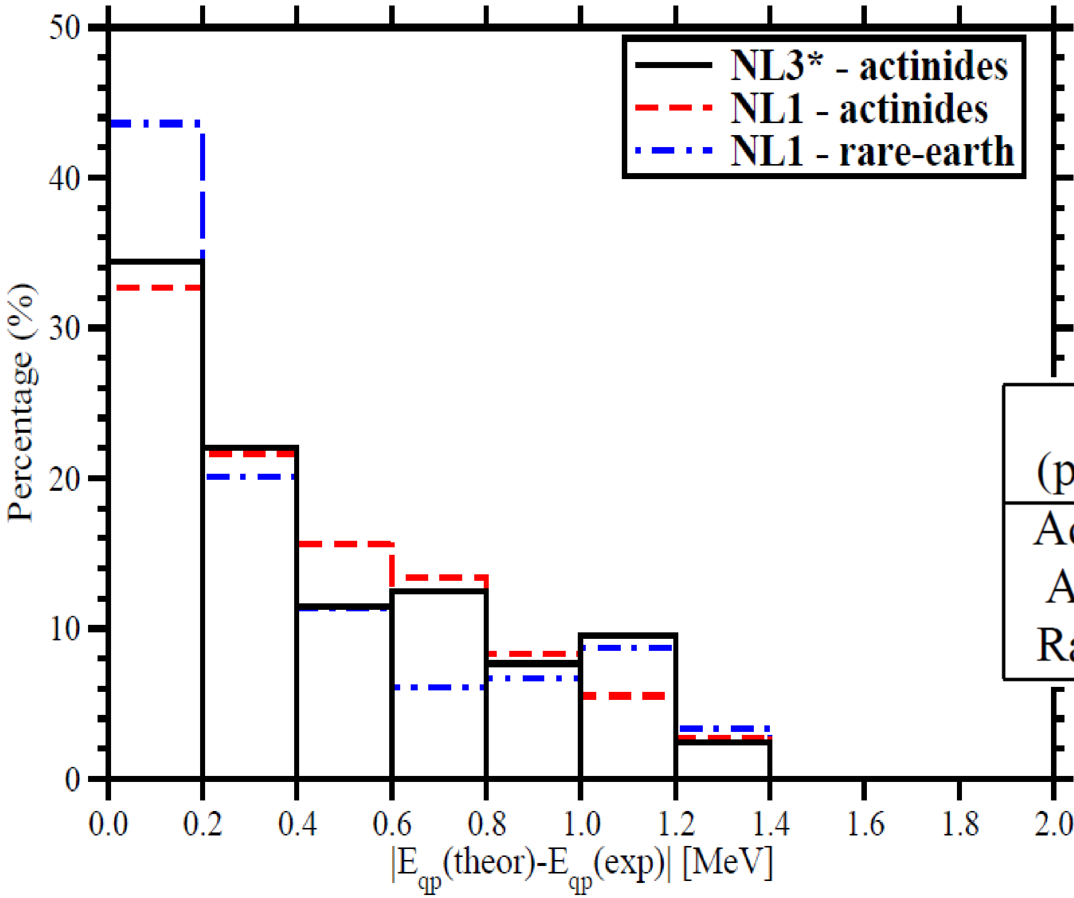

The description of deformed states at DFT level is better than spherical ones by a factor 2-3 (and by a factor ~1(neutron) and ~2 (proton) as compared with spherical PVC calculations)

Region (parametrization)	calculated states (#)	compared states (#)
Actinides (NL3*)	415	209
Actinides (NL1)	444	217
Rare-earth (NL1)	360	149

Triaxial CRHB; fully self-consistent blocking, time-odd mean fields included, NL3*, Gogny D1S pairing, AA and S.Shawaqfeh, PLB 706 (2011) 177

Two sources of deviations:

1. Low effective mass (stretching of the energy scale)
2. Wrong relative energies of the states

Deformed one-quasiparticle states: covariant and non-relativistic DFT description versus experiment

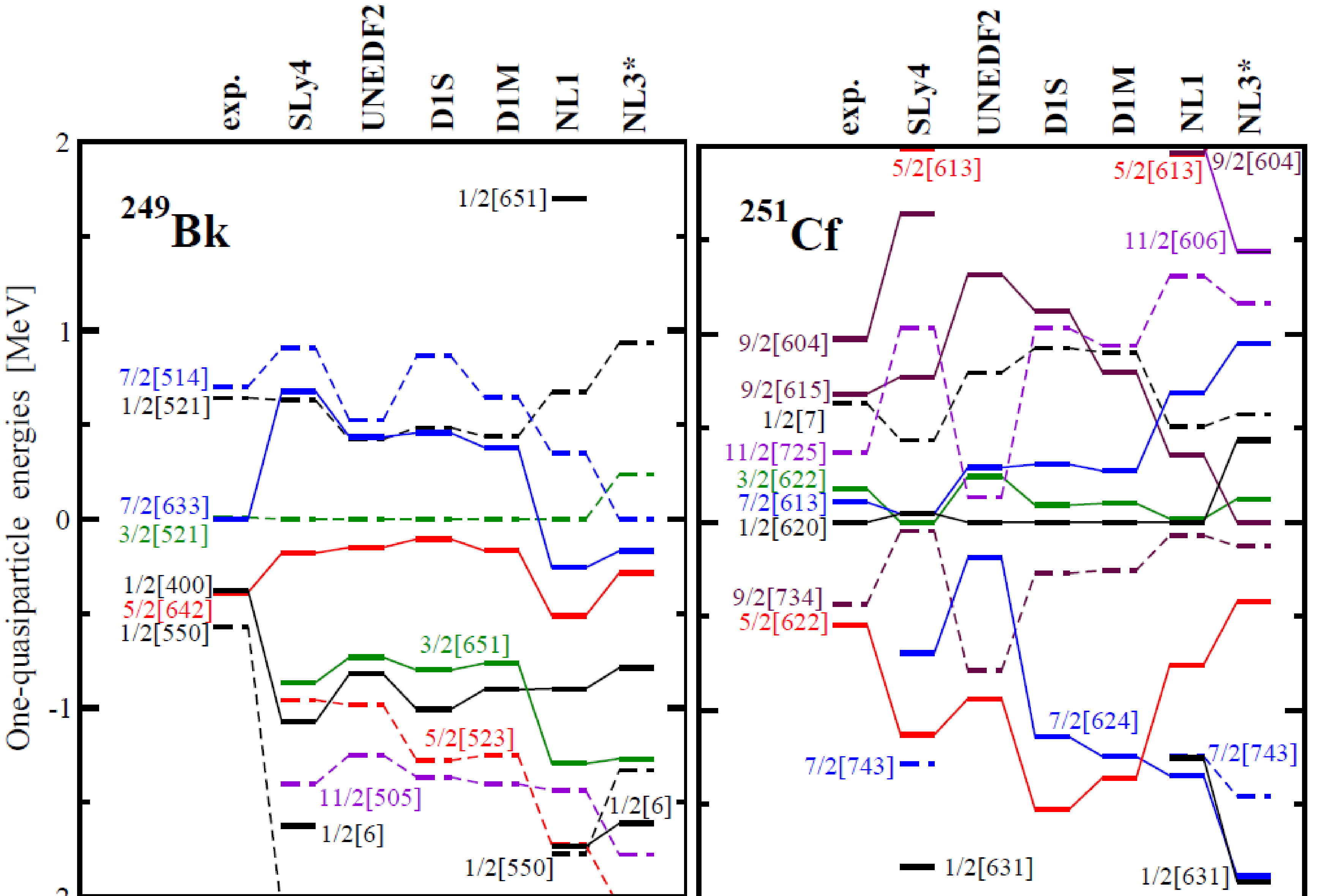

J.Dobaczewski, AA, et al, NPA, in press

Impact of quasiparticle-vibration coupling on the spectra

NL3* covariant energy density functional

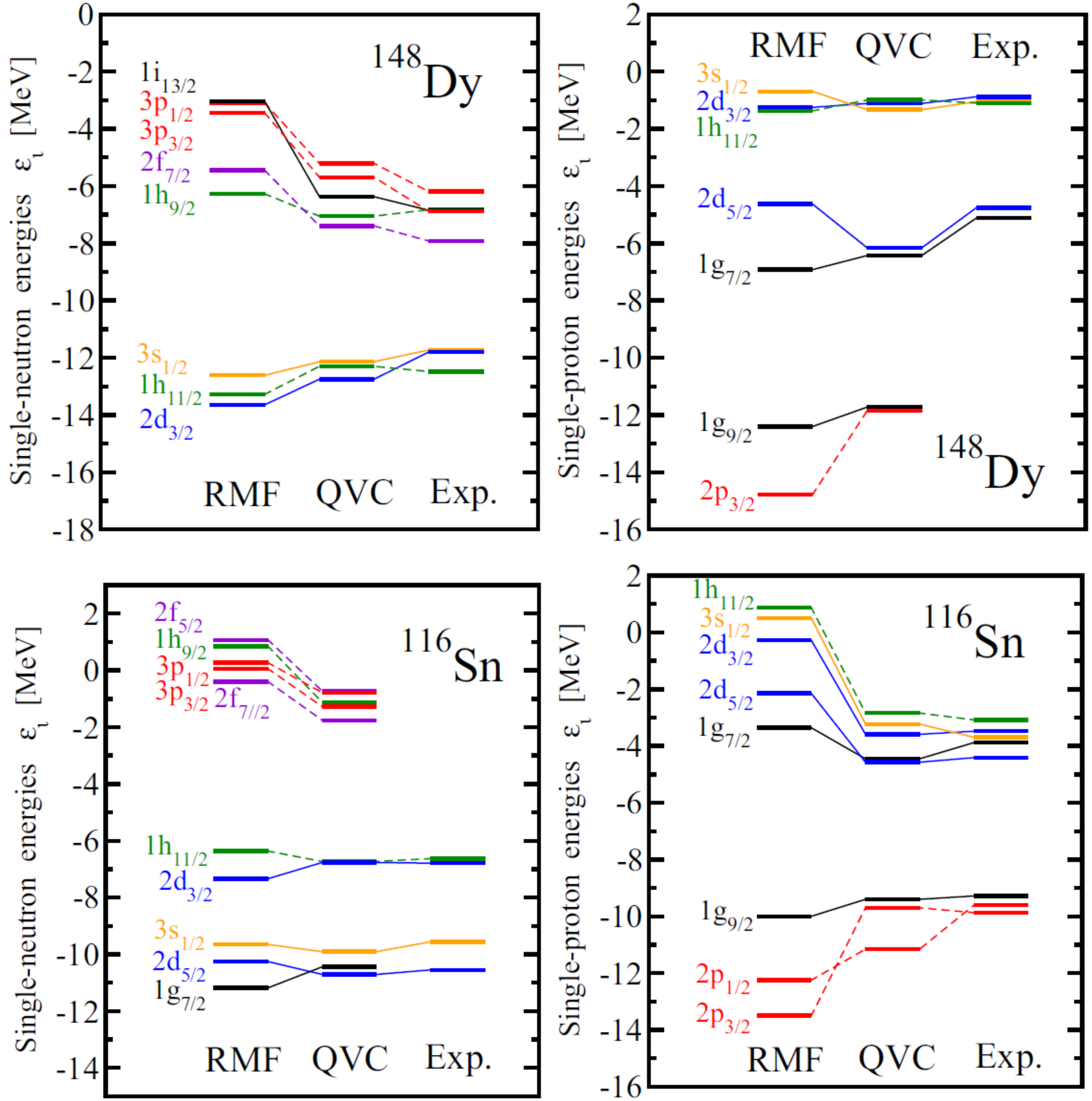

AA, E.Litvinova, PRC 92, 044317 (2015)

Relativistic quasiparticle-vibration coupling calculations: **(1)** the NL3* functional and **(2)** no tensor interaction

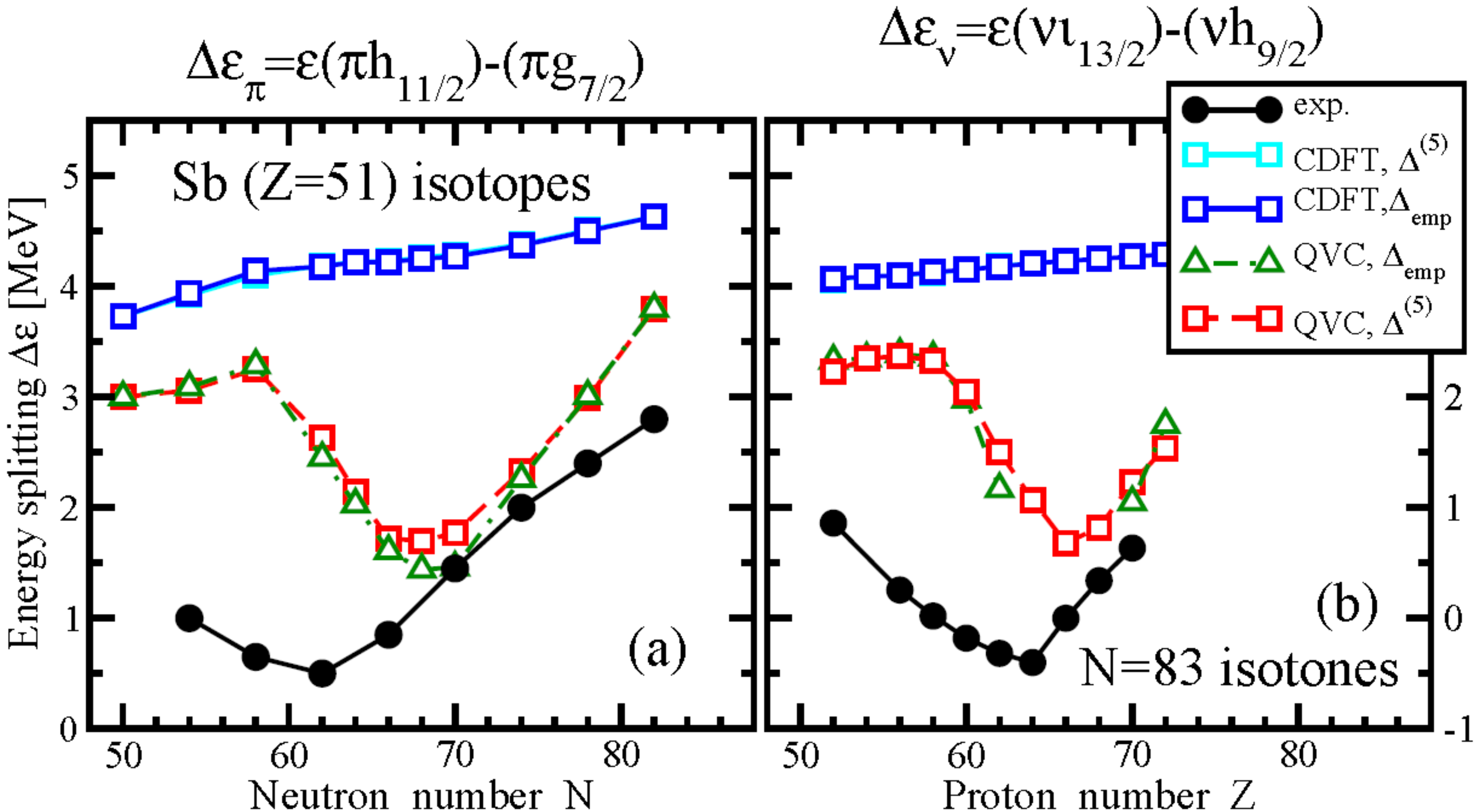

Our analysis clearly indicates that both QVC and tensor interaction act in the same direction and reduce the discrepancies between theory and experiment for the splittings of interest. As a consequence of this competition, the effective tensor force has to be weaker as compared with earlier estimates.

Fragmentation of the single-particle strength

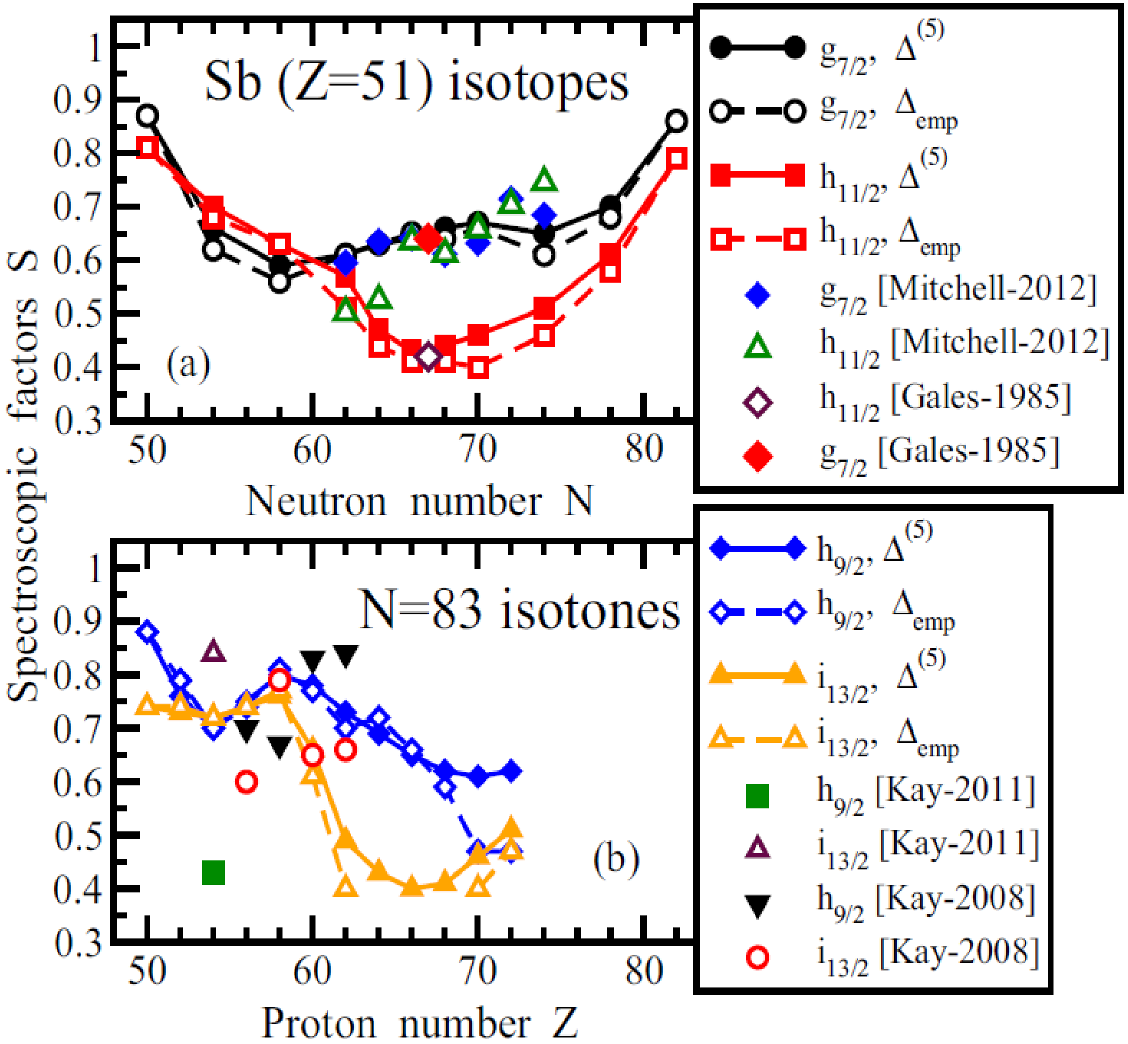

J. P. Schiffer et al, PRL 92, 162501 (2004) – the states of interest are single-particle ones (S=1)

J. Mitchell, PhD thesis, University of Manchester, (2012) – strong fragmentation of the single-particle strength (cannot be accounted at the DFT level)

M. Conjeaud et al, NPA 117, 449 (1968) and O. Sorlin Prog. Part. Nucl. Phys. 61, 602 (2008) also support low S~0.5 for $\pi h_{11/2}$ state in mid-shell Sb isotopes

B.P.Kay et al, PRC 84, 024325 (2011)
PLB 658, 216 (2008)

Quasiparticle-vibration coupling versus tensor force

The definition of the strength of the tensor interaction by means of the fitting to the energies of the dominant single-quasiparticle states in odd-mass nuclei is flawed without accounting for the effects of quasiparticle-vibration coupling.

Example of generic problems of many functionals: Deformed shell gaps at N=152 and Z=100

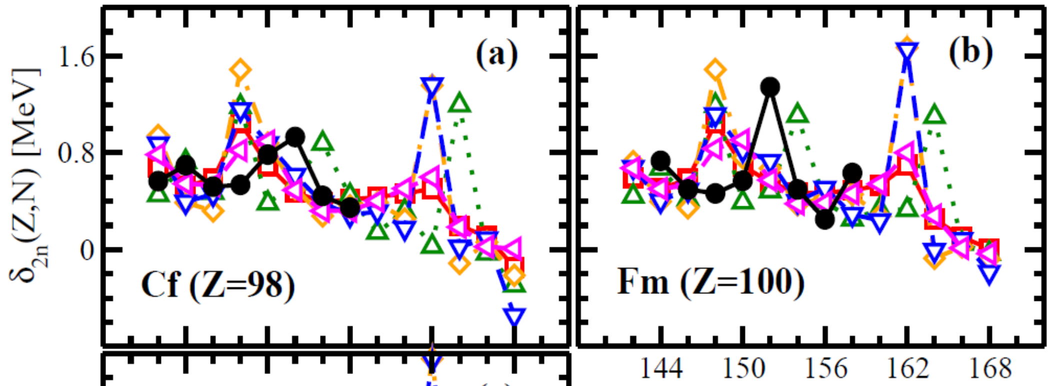

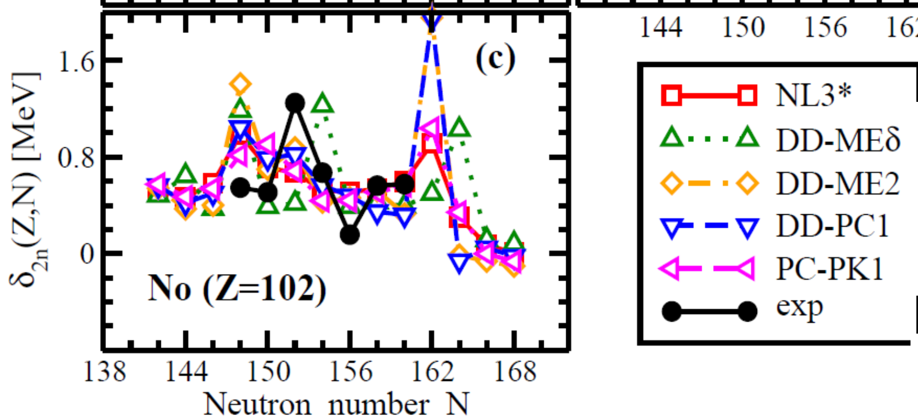

$$\delta_{2p}(N,Z) = S_{2p}(N,Z) - S_{2p}(N,Z+2),$$

$$\delta_{2n}(N,Z) = S_{2n}(N,Z) - S_{2n}(N+2,Z).$$

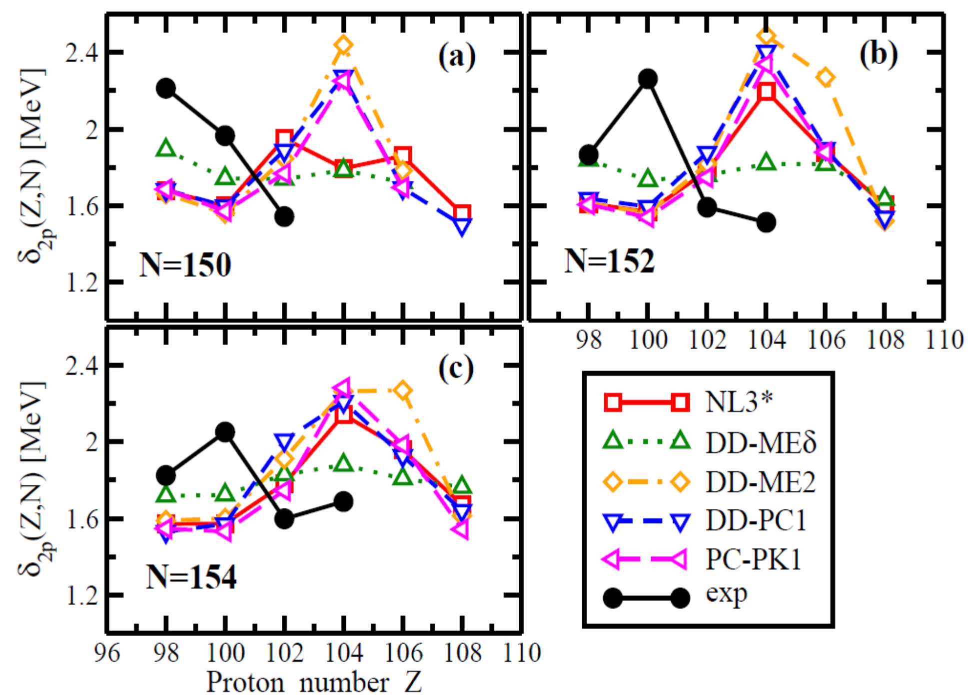

Towards spectroscopic quality DFT:

1. Improvement of the functionals at the DFT level

2. Accounting of (quasi)particle-vibration coupling

3. Inclusion of tensor interaction (not clear at this point)

The impact of the uncertainties in the single-particle energies on other observables:
example of rotating nuclei

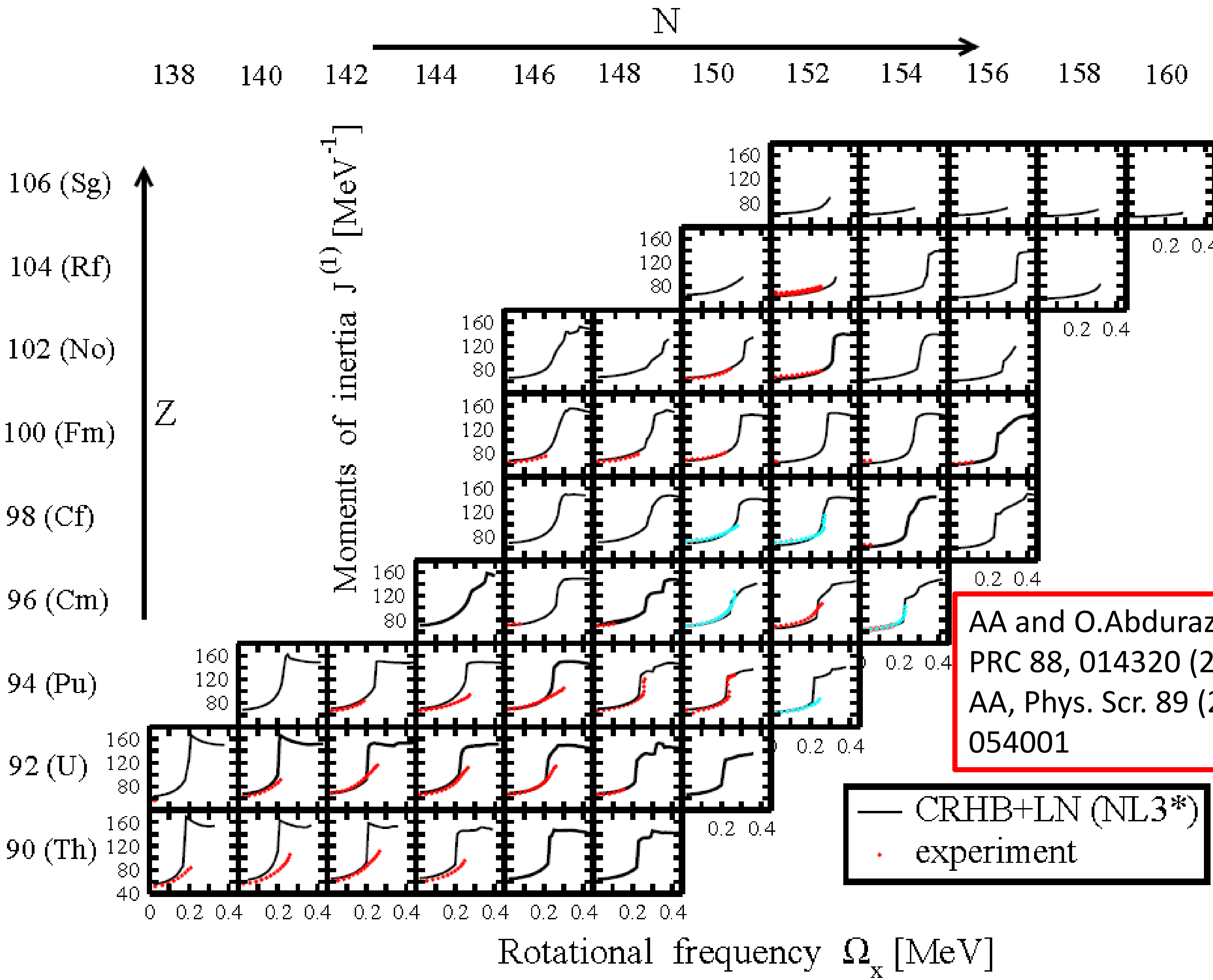

AA and O.Abdurazakov, PRC 88, 014320 (2013)
AA, Phys. Scr. 89 (2014) 054001

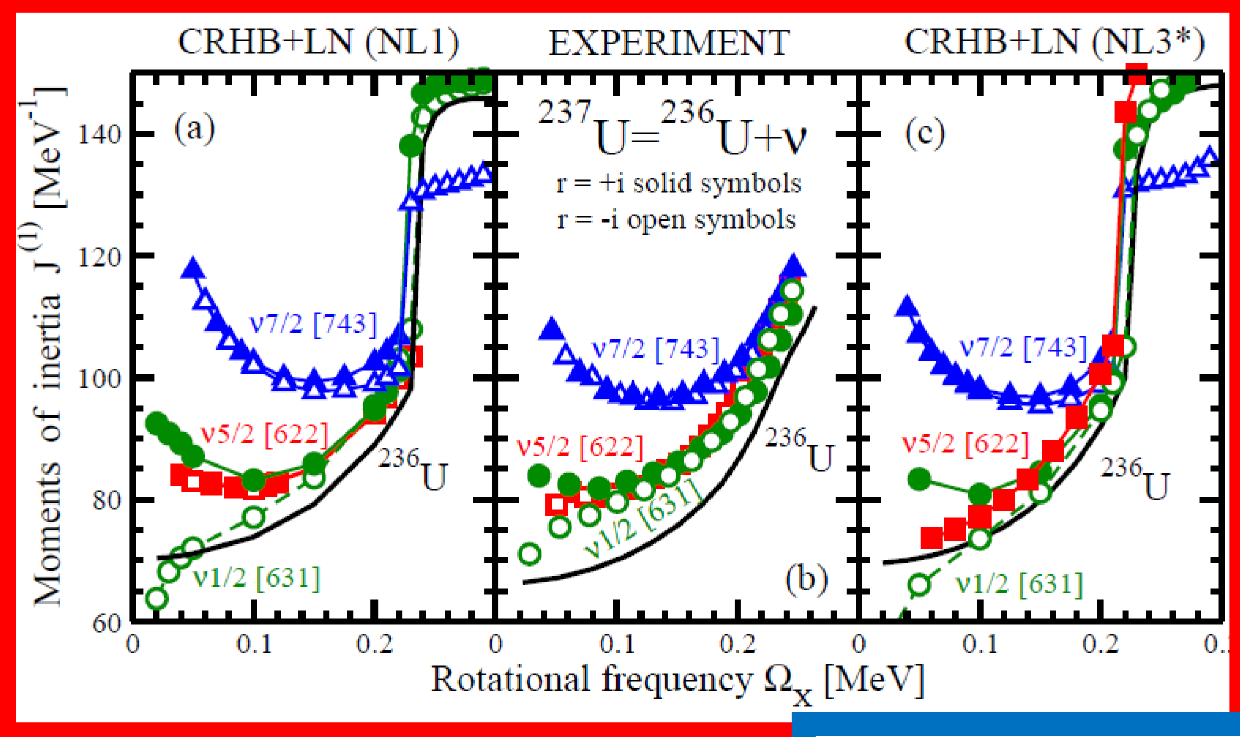

Increase of $J^{(1)}$ in odd-proton nucleus as compared with even-even ^{240}Pu is due to blocking which includes:

(a) Decrease of proton or neutron pairing

(b) Alignment properties of blocked proton or neutron state

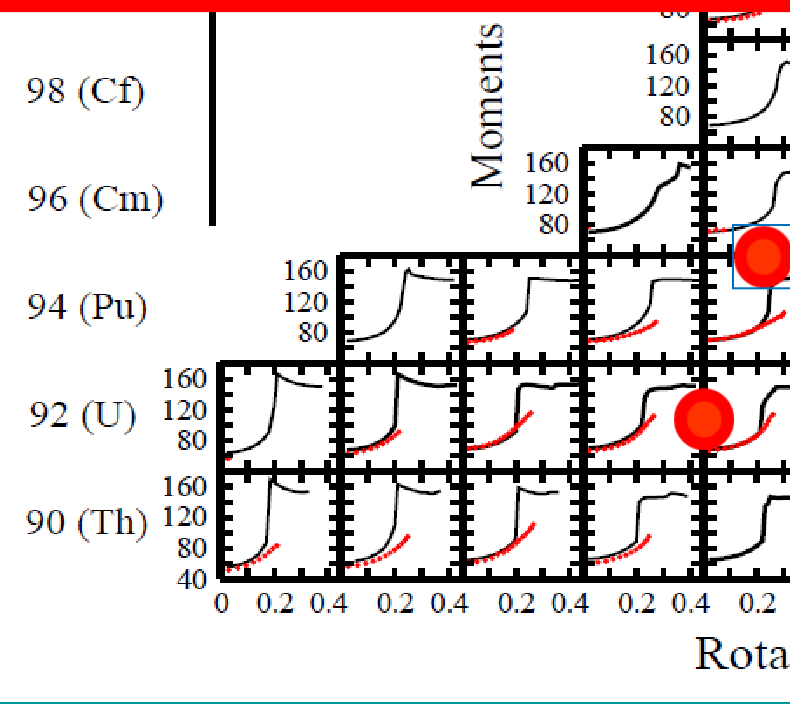

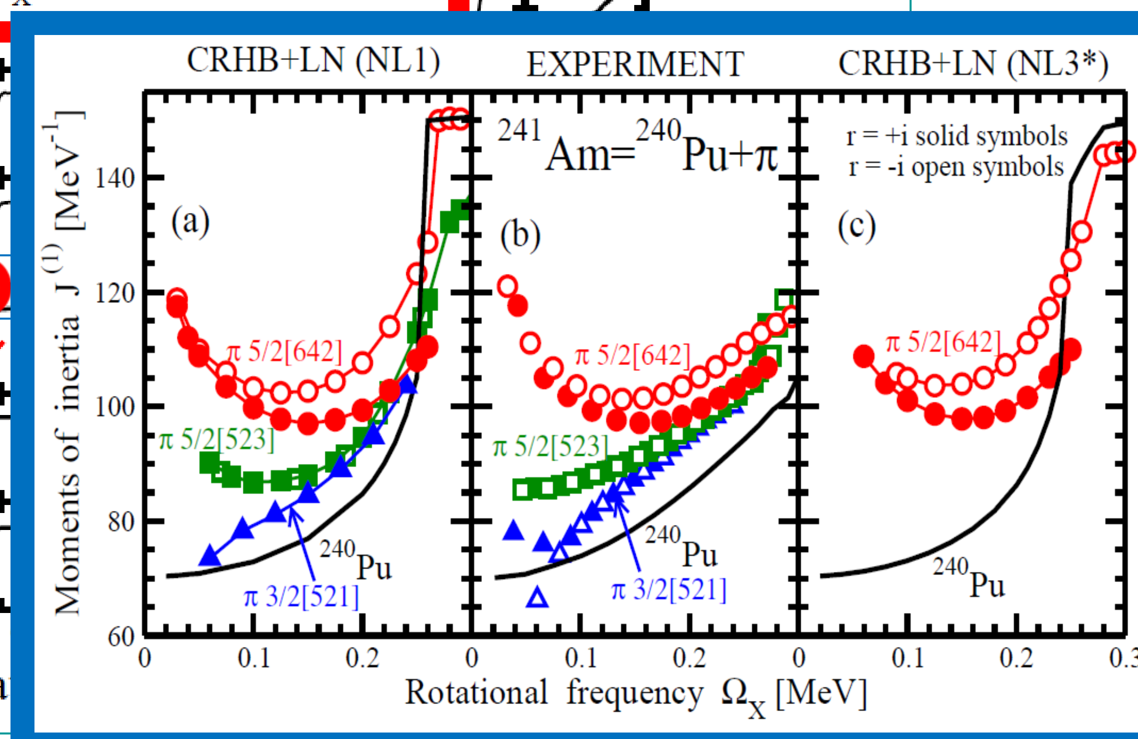

Paired band crossings: CRHB+LN versus CSM+PNP

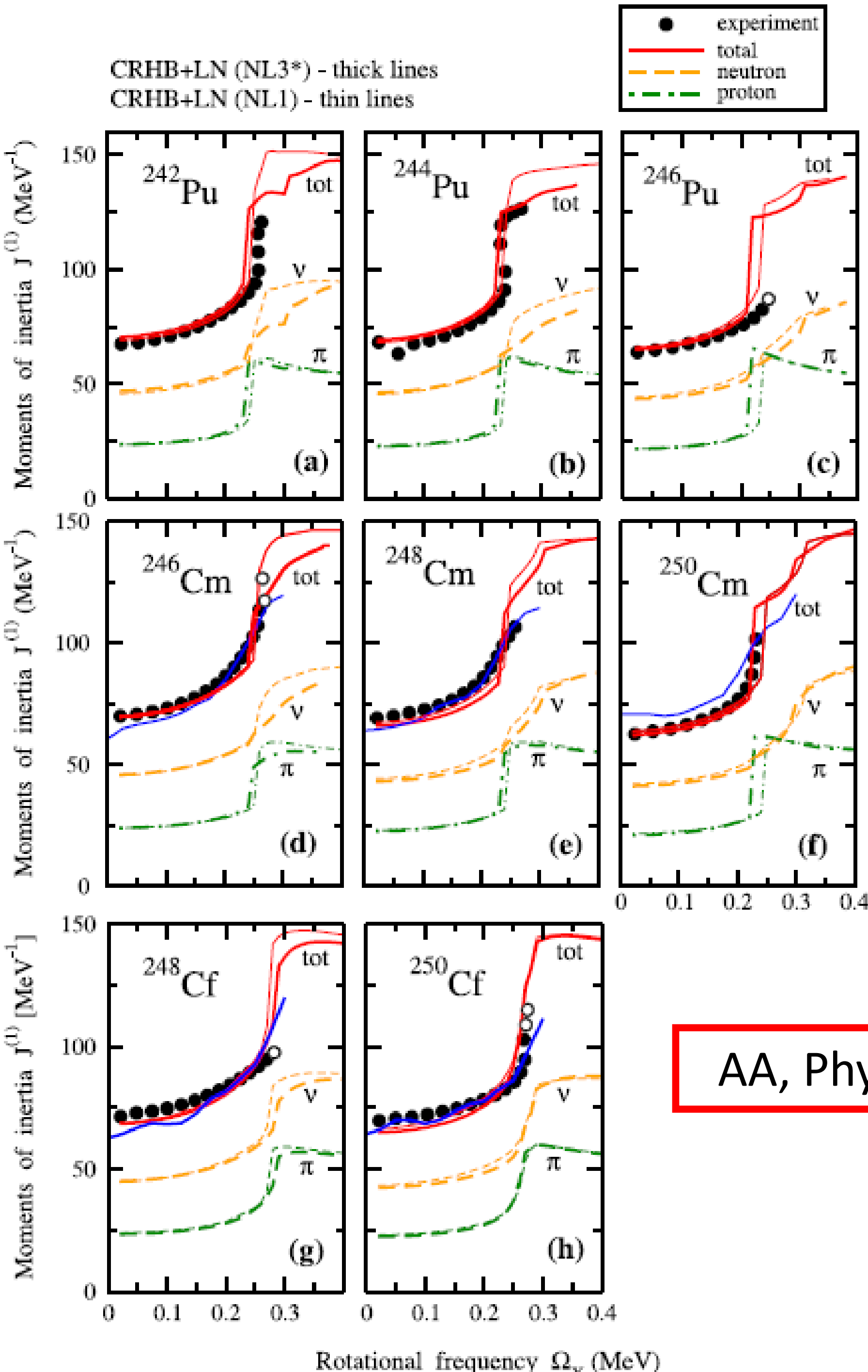

New exp. data
S. Hota, PLB 739, 13 (2014)

CSM+PNP (Z.-H.Zhang et al, PRC 85, 014324 (2012)).
Careful fit of:
- Parameters of Nilsson potential to the energies of the single-particle states
- Different pairing strength in even-even and odd nuclei
- Experimental deformations

AA, Phys. Scr. 89 (2014) 054001

CRHB+LN provides more consistent and more accurate description of experimental data than CSM+PNP

Spectroscopy of ^{240}U

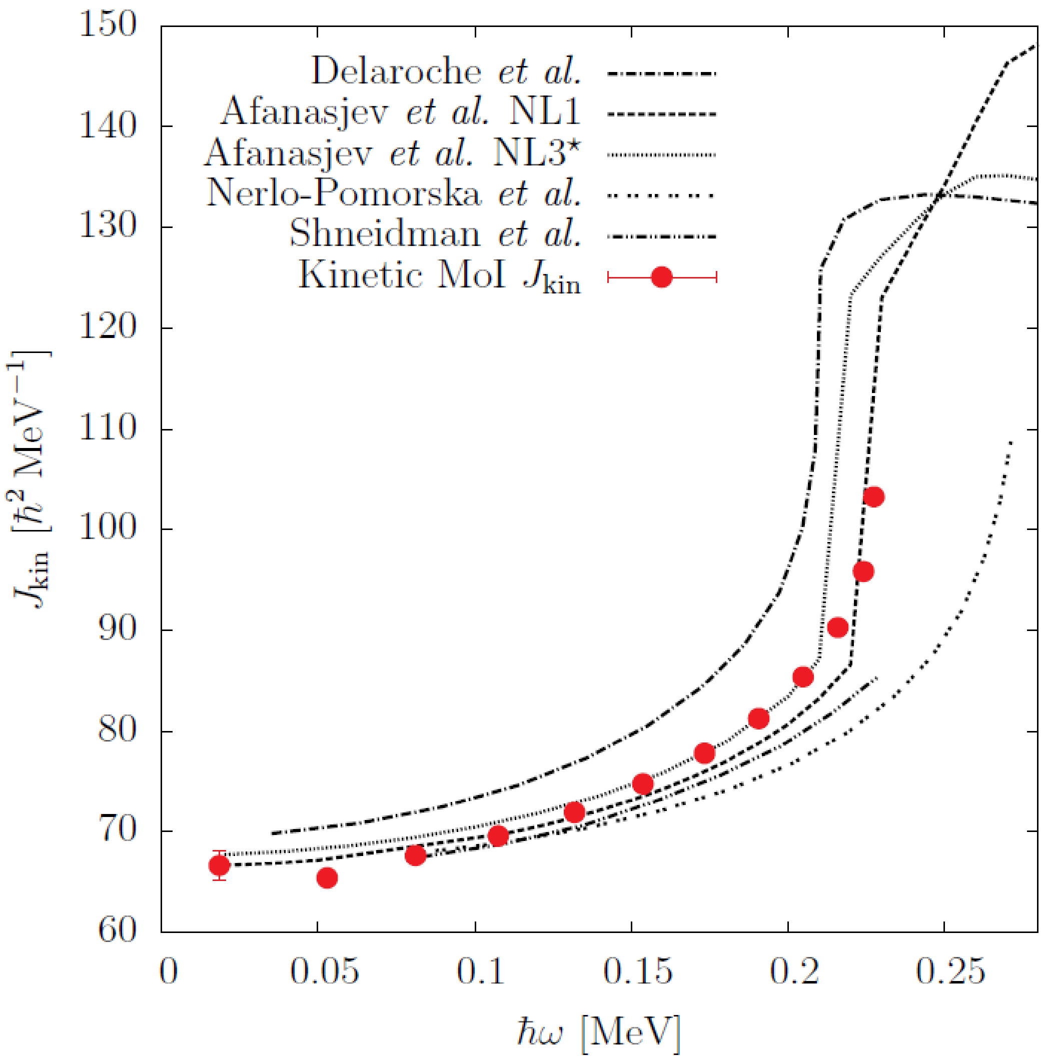

B. Birkenbah et al, Phys. Rev. C 92, 044319 (2015)

Conclusions:

1. The accuracy and uncertainties in the description of different physical observables are quantified. State-of-the-art functionals are benchmarked.

2. Theoretical uncertainties for many physical observables are most pronounced in transitional nuclei (due to soft potential energy surfaces) and in the regions of transition between prolate and oblate shapes. This is where the details depend on the accuracy of the description of energies of the single-particle states.

3. Further improvement of CEDF requires the use of the information on the energies of the single-particle states. Hopefully this will also reduce “random” (in the [Z,N] plane) component of theoretical uncertainties.